



**UNIVERSIDAD DE INVESTIGACIÓN DE
TECNOLOGÍA EXPERIMENTAL YACHAY**

Escuela de Ciencias Físicas y Nanotecnología

**TÍTULO: X-ray photoelectron spectroscopy in carbon-based
nanomaterials**

Trabajo de integración curricular presentado como requisito para
la obtención del título de Ingeniero en Nanotecnología

Autor:

Ibarra Barreno Carolina Mishell

Tutor:

Dr. rer. nat. Chacón Torres Julio C.

Urcuquí, diciembre de 2020

Urcuquí, 13 de noviembre de 2020

SECRETARÍA GENERAL
(Vicerrectorado Académico/Cancillería)
ESCUELA DE CIENCIAS FÍSICAS Y NANOTECNOLOGÍA
CARRERA DE NANOTECNOLOGÍA
ACTA DE DEFENSA No. UITEY-PHY-2020-00022-AD

A los 13 días del mes de noviembre de 2020, a las 10:30 horas, de manera virtual mediante videoconferencia, y ante el Tribunal Calificador, integrado por los docentes:

Presidente Tribunal de Defensa	Dra. GONZALEZ VAZQUEZ, GEMA , Ph.D.
Miembro No Tutor	Dr. MOWBRAY , DUNCAN JOHN , Ph.D.
Tutor	Dr. CHACON TORRES, JULIO CESAR , Ph.D.

El(la) señor(ita) estudiante **IBARRA BARRENO, CAROLINA MISHELL**, con cédula de identidad No. **1725270233**, de la **ESCUELA DE CIENCIAS FÍSICAS Y NANOTECNOLOGÍA**, de la Carrera de **NANOTECNOLOGÍA**, aprobada por el Consejo de Educación Superior (CES), mediante Resolución **RPC-SO-13-No.156-2015**, realiza a través de videoconferencia, la sustentación de su trabajo de titulación denominado: **X-RAY PHOTOELECTRON SPECTROSCOPY IN CARBON-BASED NANOMATERIALS**, previa a la obtención del título de **INGENIERO/A EN NANOTECNOLOGÍA**.

El citado trabajo de titulación, fue debidamente aprobado por el(los) docente(s):

Tutor Dr. CHACON TORRES, JULIO CESAR , Ph.D.

Y recibió las observaciones de los otros miembros del Tribunal Calificador, las mismas que han sido incorporadas por el(la) estudiante.

Previamente cumplidos los requisitos legales y reglamentarios, el trabajo de titulación fue sustentado por el(la) estudiante y examinado por los miembros del Tribunal Calificador. Escuchada la sustentación del trabajo de titulación a través de videoconferencia, que integró la exposición de el(la) estudiante sobre el contenido de la misma y las preguntas formuladas por los miembros del Tribunal, se califica la sustentación del trabajo de titulación con las siguientes calificaciones:

Tipo	Docente	Calificación
Miembro Tribunal De Defensa	Dr. MOWBRAY , DUNCAN JOHN , Ph.D.	9,5
Tutor	Dr. CHACON TORRES, JULIO CESAR , Ph.D.	10,0
Presidente Tribunal De Defensa	Dra. GONZALEZ VAZQUEZ, GEMA , Ph.D.	9,5

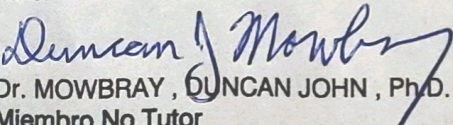
Lo que da un promedio de: **9.7 (Nueve punto Siete)**, sobre 10 (diez), equivalente a: **APROBADO**

Para constancia de lo actuado, firman los miembros del Tribunal Calificador, el/la estudiante y el/la secretario ad-hoc.


IBARRA BARRENO, CAROLINA MISHELL
Estudiante


Dra. GONZALEZ VAZQUEZ, GEMA , Ph.D.
Presidente Tribunal de Defensa


Dr. CHACON TORRES, JULIO CESAR , Ph.D.
Tutor


Dr. MOWBRAY , DUNCAN JOHN , Ph.D.
Miembro No Tutor

Karla Alarcon Felix

ALARCON FELIX, KARLA ESTEFANIA
Secretario Ad-hoc

AUTORÍA

Yo, **Carolina Mishell Ibarra Barreno**, con cédula de identidad 1725270233, declaro que las ideas, juicios, valoraciones, interpretaciones, consultas bibliográficas, definiciones y conceptualizaciones expuestas en el presente trabajo; así como, los procedimientos y herramientas utilizadas en la investigación, son de absoluta responsabilidad de el/la autora (a) del trabajo de integración curricular. Así mismo, me acojo a los reglamentos internos de la Universidad de Investigación de Tecnología Experimental Yachay.

Urcuquí, diciembre 2020.



Carolina Mishell Ibarra Barreno

CI: 1725270233

AUTORIZACIÓN DE PUBLICACIÓN

Yo, **Carolina Mishell Ibarra Barreno**, con cédula de identidad 1725270233, cedo a la Universidad de Investigación de Tecnología Experimental Yachay, los derechos de publicación de la presente obra, sin que deba haber un reconocimiento económico por este concepto. Declaro además que el texto del presente trabajo de titulación no podrá ser cedido a ninguna empresa editorial para su publicación u otros fines, sin contar previamente con la autorización escrita de la Universidad.

Asimismo, autorizo a la Universidad que realice la digitalización y publicación de este trabajo de integración curricular en el repositorio virtual, de conformidad a lo dispuesto en el Art. 144 de la Ley Orgánica de Educación Superior

Urququí, diciembre 2020.



Carolina Mishell Ibarra Barreno

CI: 1725270233

Acknowledgements

This research project was possible due to all the support of Dr. Julio Chacón. I would like to thank for giving me the opportunity with this project, for all his help, teaching and patience along this year and a half that we worked together. It has been an enriching experience as student and researcher. I learnt a lot from each class, laboratory and conversation that we had. Also, I would like to thank for the help of Claudia Kroeckel, Luis Corredor, Carla Bittencourt and Carlos Reinoso who were responsible for the synthesis methods and XPS measurements in Mons University and Yachay Tech University for this project.

In addition, I also would like to thank to: Dra. Gema González, Dra. Mayra Peralta, Dr. Juan Saucedo and Dra. Sarah Briceño who helped, taught and inspired me along my college years. Also, I would like to thank to my mother Cecilia Barreno and my brother Diego Ibarra who always supported me in all the possible ways that they could have done it.

At this point, I would like to mention my friends who shared with me good and bad times: Samantha Naranjo, Raúl Hidalgo, Ariana Rivera, Lady Ríos, Patricio Paredes, Kerly León, Michael Jiménez, Nicolás Marin, Vanessa Hinojosa, Cristina Mina, Romina Bermeo, Jonathan Recalde, José Durán and also to my friends: Nohely Rivilla, Sharon Masabanda, Tefa Chávez, Daniela Bastidas and Ivonne Chávez. Finally, I would like to thank to my boyfriend and his family, thank you Mateo Narváez for making this experience much better with your company and love.

Carolina Mishell Ibarra Barreno

Resumen

El grafeno y los nanotubos de carbono de paredes múltiples (MWCNTs) han generado mucho interés en el campo de la nanotecnología por su alta conductividad y fuerza mecánica. Por un lado, el grafeno tiene una baja reactividad química debido a la estabilidad en sus enlaces y debe ser funcionalizado para poder aprovechar mejor sus propiedades. Por otro lado, los MWCNTs pueden presentar contaminantes en la estructura tubular después del proceso de síntesis. Esta investigación tiene dos objetivos: 1) analizar la funcionalización e interacciones químicas en grafeno dopado con potasio y expuesto a O₂, H₂O y moléculas de yodo hexano (muestras: K@Gr+O₂, K@Gr+H₂O and K@Gr+Hex) y 2) analizar la calidad de MWCNTs sintetizados en la Universidad Yachay Tech por medio de espectroscopia de fotoelectrones emitidos por rayos X (XPS). Esta técnica de caracterización permite determinar de forma precisa la composición elemental y enlaces químicos en la superficie de la muestra, ideal para el análisis de funcionalización y calidad de cualquier material. Los resultados del XPS para grafeno mostraron un material de alta calidad (57 - 73% de carbono) funcionalizado no covalentemente con potasio (30.84% de carbono por potasio, muestra K@Gr+H₂O) mediante interacciones catión – orbital π (Fuerza de Coulomb), con grupos funcionales (3.6 - 7.63% de carbono por grupo funcional como: epóxidos, carbonilos, ácidos carboxílicos) y una ligera oxidación (10 - 20%) debido al proceso de transferencia con polimetilmetacrilato (PMMA). Para las muestras K@Gr+O₂ y K@Gr+H₂O, los iones de potasio son responsables por transferencia de carga mientras que los óxidos de potasio son responsables por la migración de oxígenos (de los grupos funcionales adheridos a la superficie), sin dañar la estructura. La muestra K@Gr+Hex mostró una recuperación de la estructura de grafeno aún después del proceso de dopaje debido al ambiente con moléculas de yodo hexano. Los resultados de XPS para los MWCNTs mostraron un material altamente puro (98% de carbono) con hibridación sp², comportamiento metálico y baja concentración de oxígeno (1.2%) debido a la descomposición del sustrato de CaCO₃. Finalmente, el proceso de dopaje y funcionalización de grafeno es el primer abordaje para cambiar el comportamiento inerte hacia un material más hidrofílico y biocompatible sin introducir defectos o romper la simetría de la estructura por medio del dopaje de cationes y grupos funcionales. Los MWCNTs fueron sintetizados con alta calidad sin presencia de contaminantes, lo cual representa una ventaja para evitar pasos extra de purificación que podría dañar la estructura tubular. Los resultados son de gran importancia para confirmar el método de síntesis de un material adecuado para aplicaciones tecnológicas como dispositivos electrónicos o potenciales biosensores.

Palabras clave: XPS, grafeno, potasio, grupos funcionales, PMMA, MWCNTs, CaCO₃.

Abstract

Graphene and multiwalled carbon nanotubes (MWCNTs) have generated interest in the nanotechnology given their high electrical conductivity and mechanical strength. However, graphene has low chemical reactivity by its stable bonds unless it is functionalized to take advantage of its properties. MWCNTs have problems by the contaminants presence in the structure after the synthesis. This investigation has two objectives: 1) to analyze the functionalization and chemical interaction of potassium-doped graphene exposed to O₂, H₂O and hexyliodide molecules (K@Gr+O₂, K@Gr+H₂O and K@Gr+Hex samples) and 2) to analyze the quality of MWCNTs synthesized at Yachay Tech University by means of X-ray photoelectron spectroscopy (XPS) which is a precise technique to determine the elemental composition and chemical bonding on a surface sample, ideal for the analysis of functionalization and quality of a material. The XPS results for graphene show high quality material (57 - 73% of carbon) non covalent functionalized with potassium (30.84% of carbon per potassium in K@Gr+H₂O) through cation- π interactions (Coulombic forces), functional groups (3.6 - 7.63% of carbon per functional group as: epoxy, carbonyl, carboxylic acid groups) and a slight oxidation (10 - 20%) due to the transferring process with polymethylmethacrylate (PMMA). For K@Gr+O₂ and K@Gr+H₂O samples, potassium ions are responsible for charge transfer effects whereas potassium oxides become responsible for the migration of oxygen attached molecules to the graphene surface without affecting the structure. The K@Gr+Hex sample shows a recovery of the graphene structure after the doping process due to the hexyliodide environment. The XPS characterization results for MWCNTs show a highly pure material (98% of carbon) with a sp² hybridization, metallic behavior and low concentration of oxygen (1.2%) due to the decomposition of CaCO₃ substrate. Finally, the doping and functionalization of graphene is a first approach for changing its inert behavior into a hydrophilic and biocompatible novel material without introducing defects or breaking its structure through cation doping with functional groups. The MWCNTs were high quality synthesized without contaminants which is an advantage to avoid extra process that might destroy the structure. These outcomes are of high importance to confirm the synthesis of material suitable for technological applications as electronic devices or potential biosensors.

Keywords: XPS, graphene, potassium, functional groups, PMMA, MWCNTs, CaCO₃.

Contents

List of Figures	xvi
List of Tables	xviii
1 Introduction	1
1.1 State of the art in Nanotechnology	1
2 Theoretical Background	5
2.1 Nanomaterials	5
2.1.1 Graphene	6
2.1.2 Multiwalled carbon nanotubes	11
2.1.3 Funcionalization of graphene	14
2.2 Characterization Techniques	16
2.2.1 X-ray Photoelectron Spectroscopy (XPS)	16
2.2.2 XPS in graphene and multiwalled carbon nanotubes	24
3 Motivation and Research objectives	27
4 Methodology	29
4.1 Synthesis of functionalized graphene samples	29
4.2 Synthesis of CVD multiwalled carbon nanotubes	32
4.3 XPS measurements	33
4.4 Fitting Methodology	34
4.4.1 Calibration of a XPS spectra	35

4.4.2	Peak deconvolution	36
5	Results & Discussion	39
5.1	Graphene samples	39
5.1.1	Elemental analysis of graphene samples	39
5.1.2	High resolution analysis of graphene pristine	44
5.1.3	High resolution analysis of potassium-doped graphene exposed to O ₂	48
5.1.4	High resolution analysis of potassium-doped graphene exposed to H ₂ O	53
5.1.5	High resolution analysis of potassium-doped graphene exposed to hexylo- dide	58
5.2	MWCNTs sample	63
5.2.1	Elemental analysis of MWCNTs sample	63
5.2.2	High resolution analysis of MWCNTs	63
6	Conclusions & Outlook	69
A	XPS fitting parameters for graphene and MWCNTs samples	73
	Bibliography	79

List of Figures

2.1	Graphene representation of its orbitals and network	7
2.2	Graphene scheme in real and reciprocal space	8
2.3	Conduction and valence bands at symmetry points in reciprocal space for graphene	9
2.4	Representation of CNTs structures made on Avogadro software	11
2.5	Chiral vector which defines the geometrical parameters for CNTs ¹	12
2.6	Armchair and zigzag nanotubes	13
2.7	Photoelectron process representation.	17
2.8	Three step model explaining the photoelectron emission process	18
2.9	Schematic representation of XPS equipment	21
2.10	Survey and high-resolution spectra for carbon sample	25
4.1	Synthesis processes for graphene samples	31
4.2	Synthesis process for MWCNTs. Sketch adapted ²	32
4.3	XPS equipment at MONS University used for measuring graphene samples. . . .	33
4.4	XPS equipment at Yachay Tech University used for measuring MWCNTs samples.	34
4.5	Au 4f spectrum for calibration process	36
5.1	XPS spectra of surveys from graphene samples	40
5.2	Fitting for C1s and O1s regions from Gr sample	45
5.3	Fitting for C1s and O1s regions from K@Gr+O ₂ sample	49
5.4	Fitting for C1s and O1s regions from K@Gr+H ₂ O sample	54
5.5	Fitting for C1s and O1s regions from K@Gr+Hex sample	59
5.6	Survey spectrum for MWCNTs pristine	64
5.7	Fitting for C1s and O1s regions from MWCNTs sample	66

List of Tables

5.1	Atomic percentages of the elements found at the surface of the four different samples	42
5.2	Assignment of peaks for C1s and O1s regions for graphene pristine sample. . . .	47
5.3	Assignment of peaks for C1s and O1s regions for potassium-doped graphene sample exposed to air.	51
5.4	Assignment of peaks for C1s and O1s regions for potassium-doped graphene sample exposed to water.	56
5.5	Assignment of peaks for C1s and O1s regions for potassium-doped graphene sample exposed to hexyliodide.	61
5.6	Atomic percentages of the elements present at MWCNTs pristine samples	65
5.7	Assignment of peaks for C1s and O1s regions for MWCNTs sample	67
A.1	Parameters for the peak deconvolution on C1s region for Gr sample	74
A.2	Parameters for the peak deconvolution on O1s region for Gr sample	74
A.3	Parameters for the peak deconvolution on C1s region for K@Gr+O ₂ sample	75
A.4	Parameters for the peak deconvolution on O1s region for K@Gr+O ₂ sample	75
A.5	Parameters for the peak deconvolution on C1s region for K@Gr+H ₂ O sample	76
A.6	Parameters for the peak deconvolution on O1s region for K@Gr+H ₂ O sample	76
A.7	Parameters for the peak deconvolution on C1s region for K@Gr+Hex sample	77
A.8	Parameters for the peak deconvolution on O1s region for K@Gr+Hex sample	77
A.9	Parameters for the peak deconvolution on C1s region for MWCNTs sample	78
A.10	Parameters for the peak deconvolution on O1s region for MWCNTs sample	78

Chapter 1

Introduction

1.1 State of the art in Nanotechnology

Nanotechnology has become into one of the most important fields of science of our time, focused on the manipulation of matter at the nanoscale and also, in taking advantage of a materials' properties at the nanolevel³. The idea of nanotechnology came up for the first time in December 1959 during a talk of the physicist Professor Richard Feynman⁴. He introduced the problem of manipulating or controlling matter at very small scales but also about the great opportunity of doing it because it might lead to the development of technology at an advanced level. In this way, Prof. Feynman guided physicists to a new research field in science called, years later, Nanotechnology.

It was not until 1974 that Norio Taniguchi settled the basic concepts about Nanotechnology. His paper settled the working scale (10^{-9} meters) and also stated the main materials, devices and machines for controlling matter at the nanometer scale⁵. From this, the following works were focused on the processing of: separation, consolidation or deformation of materials in order to exploit their properties at this scale. Nevertheless, it was possible many years later to appreciate a real manipulation with techniques such as Scanning Tunneling Microscopy (STM) and Atomic Force microscopy (AFM)³. In this way, the idea of controlling matter found a solid footing and was no longer science fiction.

Nanotechnology has traveled a long way and now this is a field that depends on very sophisticated methods for the synthesis and characterization of materials by using diverse techniques. All this effort is done because the known properties for macro-systems change at the nanoscale³. In this way, the intensive and extensive properties of matter and interactions between atoms are strongly dependent on the size of the material. For instance, while the size of materials decreases, then the active surface area increases. Therefore, the material has a higher active area per unit volume which implies also a high energy surface that may allow chemical reactions and improve the efficiency of chemical processes³. This means that the synthesis methods for novel materials have been improving with time in order to obtain those size-dependent properties. This has made that nanotechnology a very successful field of study.

Likewise, nanotechnology has become a multi-disciplinary science involving related fields such as: physics, biology, chemistry, among others. For example, some of the synthesized materials are destined for: electronic devices and fabrication of nanoelectronics such as semiconductors, for medicine or biology as devices for improved therapy or diagnosis and drug delivery, for cosmetic industries in sunblocks for UV-rays, which involves all the above mentioned fields⁶. Also, they are used for reinforcements of composites, giving more resistance to materials or making a lighter, stronger or conductive product⁶. Therefore, the scope of nanotechnology can have a great impact on multiple areas of knowledge.

The development and study of novel nanomaterials have been a high intensive research topic in nanotechnology. Some researchers have focus on carbon nanomaterials due to the versatility of carbon to form different types of bonding⁷. Some of the most used carbon nanoforms are multiwalled carbon nanotubes and graphene. Carbon nanotubes were reported by many groups in 1950s. Graphene was produced in 2005 by mechanical exfoliation. Since then the research has focused on the characterization of those materials for a well description of their properties and taking advantage of the most important as electronic structure and mechanical strength⁷.

Graphene has been studied with technological purposes used as conductive electrode for many applications including solar cells, flat panel displays, touch screens, etc. Even graphene is studied as a semiconductor useful for batteries. One of the high level applications for graphene is

related to stable and controllable dope on graphene surface in order to obtain a complete control over the electronic and structural properties⁸. In this way, the surface superstructures or many functional groups are viable candidates in the search of novel graphene based materials. Moreover, the chemical changes can induce a functionalized graphene available for many fields with different purposes. All those modifications in graphene chemistry are investigated due to each modification can influence on the control of the electronic structure or chemical behavior in order to obtain suitable materials for specific applications⁹. Multiwalled carbon nanotubes also have been investigated as for example as a reinforcement for polymer composites. Their conductive and mechanical properties are useful for electronic and biological uses same as graphene.

The investigations for graphene and carbon nanotubes have been developed in order to truly understand the physical behavior of charge carriers through the surface and change their chemistry to obtain biocompatible or conductive materials. The research is still a boom and will continue for many years specially for graphene which could become the basis for new technologies⁸. Finally, the study of carbon nanomaterials is highly important for the development of new technologies based on the synthesis of suitable products with specific properties for technological applications such as the fabrication of nanoelectronics devices and bioelectronic sensors¹⁰.

Chapter 2

Theoretical Background

2.1 Nanomaterials

In general, it is considered as a nanomaterial if the materials is between 1 to 100 nanometers (or at least one of its three dimensions is at this range) of any chemical composition⁶. At this scale, it should be taken into account that there are two principal changes (internal and external) for any material related to its properties. The internal changes are related to the particular properties of the material as melting and boiling point, softness or hardness, diffusion coefficients, thermal conductivity, etc. Therefore, these changes can be treated as problems of classical mechanics caused by the size effect⁶. The external changes are related to the interaction with the external fields and the matter at the surroundings. These changes occur because when the nanomaterial is at the length of the physical phenomenons, as phonons, coherent length, irradiative wave length, screening length, etc; then causes an unexpected quantum effect and this behavior is related to quantization of electro-conductivity or due to additional low dimensional quantum states, magneto-resistance, among others⁶. This is the purpose of nanosciences, the study of those new behaviors. Therefore, it is important the study of new nanomaterials as their novel properties and mechanisms.

Along through the last decades, the developed nanomaterials are a lot and for different purposes. They can be classified depending on their structure, their nature, the synthesis method and so on. This investigation is focused on nanomaterials made of carbon atoms or carbon nanoma-

terials⁶. The carbon nanostructure has caught the attention in many and different fields. There are many nanoforms which are studied and reported. The carbon nanostructure can be used in biology field as a biosensing or in electronic devices for building semiconductors³.

The carbon element has an electronic configuration of $1s^2 2s^2 2p^2$.⁷ The atomic orbitals of 2s and 2p can be hybridized in three types: single, double and triple bonds⁷. In this way, single bond occurs when an s orbital is hybridized with three p orbitals (sp^3), this forms a tetrahedral structure. Double bond occurs when a s orbital is hybridized with two p orbitals (sp^2), this can also form trigonal planar configuration. Triple bond occurs when an s orbital is hybridized with a p orbital (sp), this forms a linear structure⁷. Moreover, the properties of the carbon-based materials are depended on the type of hybridization between carbon-carbon atoms. The form and structure define their utility.

Hence, the carbon element can form structures as diamond (sp^3), graphite (sp^2), amorphous carbon (sp^2 and sp^3), graphene (sp^2) and carbon nanotubes (sp^2), among others. For the purpose of this investigation, only graphene and carbon nanotubes are taken into account.

2.1.1 Graphene

Graphene is a honeycomb arrangement made of carbon atoms of one atom thickness. Graphene is considered as a planar sheet of carbon atoms with sp^2 hybridization⁷. In Figure 2.1, a) represents the sp^2 hybridization in a carbon-carbon bond, this hybridization is for all the carbon along the planar structure, b) is a representation of the honeycomb arrangement for a graphene layer structure. Due to its periodicity and well ordered structure, graphene is considered as true crystal in 2 dimensions (2D) and also is considered as a nanomaterial of 2D because it grows only on x and y direction⁷.

If there are more than five layers of graphene together are considered as graphite. For graphite, the interplanar interaction between layers is by Van der Waals and the interplanar distance is about 0.34 nm⁶. There are many synthesis methods to obtain graphene: micromechanical cleavage, electrochemical exfoliation, reduction of graphene oxide, liquid-phase exfoliation, among others¹¹. One of the most used methods is chemical vapor deposition (CVD) as the material grows

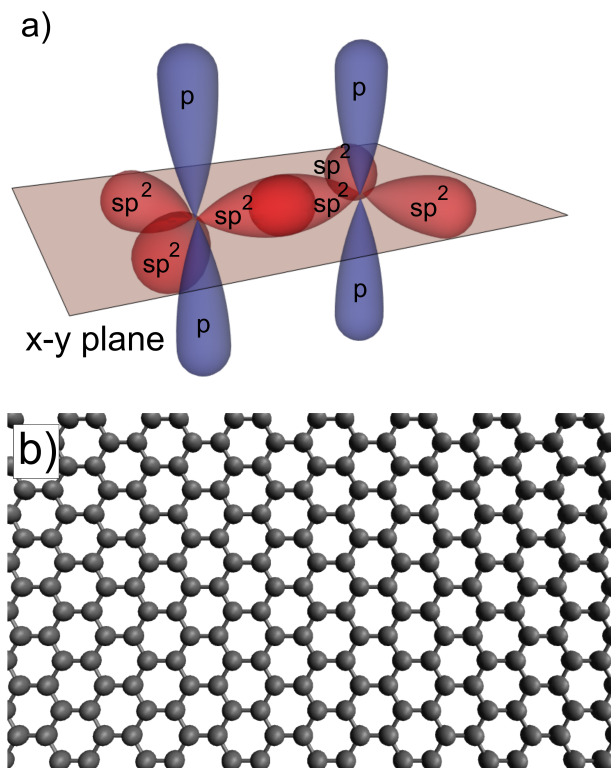


Figure 2.1: a) It is a representation for carbon with sp^2 hybridized orbitals at the x-y plane and p orbital perpendicular to them. b) It is a graphene network simulation made of Avogadro to show the well ordered structure in a hexagonal arrangement.

with high quality¹². The method is based on carbon segregation using carbon source as: methane (CH_4), ethylene (C_2H_4) or acetylene (C_2H_2) which enters to a CVD reactor. Inside of the chamber, there is a substrate which is heated to $\sim 1000^\circ C$ using a temperature controller. When the carbon source comes into vapor phase. Then, the increasing temperature is stopped, the substrate starts to cool down and the carbon atoms are deposited on a substrate as graphene layer over the substrate surface. The substrate must be a metal well oriented single crystal, otherwise it could not induce a well ordered arrangement. The temperature and cooling rate are important to determine the number of the graphene layers. After the process, the substrate with graphene is removed from the chamber and graphene can be transferred to any other substrate for appropriate purposes¹².

For graphene, the bond distance between carbon to carbon is 1.42 \AA . In real space, the unit cell are two carbon atoms (A and B) which are not equivalent, it is shown in Figure 2.2. The unitary vectors are¹³:

$$\vec{a}_1 = \frac{a_0}{2} \cdot (3, \sqrt{3}) \quad \text{and} \quad \vec{a}_2 = \frac{a_0}{2} \cdot (3, -\sqrt{3}) \quad \text{with} \quad a_0 = 1.42 \text{ \AA} \quad (2.1)$$

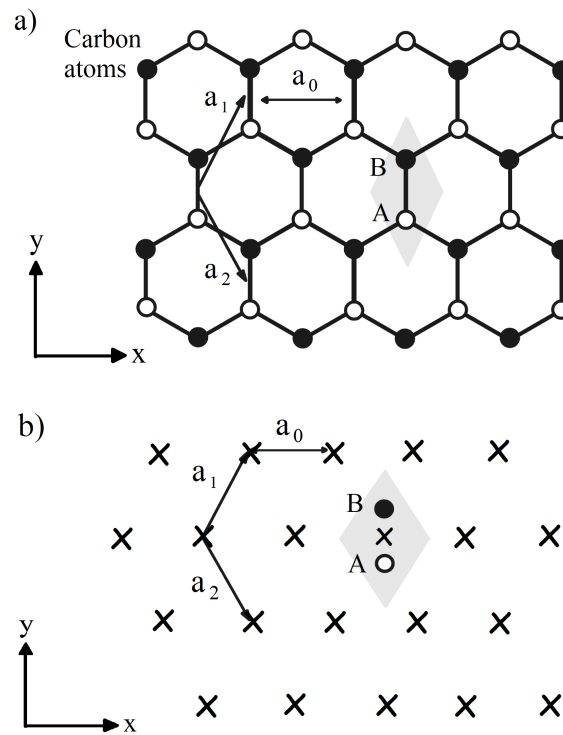


Figure 2.2: Graphene scheme. a) crystal structure of monolayer graphene, where a_1 and a_2 are the unitary vectors, a_0 is the lattice constant and A,B are two inequivalent atoms at the lattice. b) crosses indicate points of hexagonal Bravais Lattice for graphene with A and B atoms as a basis.

The reciprocal lattice vectors are:

$$\vec{b}_1 = \frac{2\pi}{3a_0} \cdot (1, \sqrt{3}) \quad \text{and} \quad \vec{b}_2 = \frac{2\pi}{3a_0} \cdot (1, -\sqrt{3}) \quad \text{with} \quad a_0 = 1.42 \text{ \AA} \quad (2.2)$$

In reciprocal space, a hexagonal lattice is also the first Brillouin zone. Given the symmetry of the zone is possible to observe symmetry points in this lattice. The center is in $(0,0)$, a corner is $K = \vec{b}_1$ and the center of a edge is $M = \frac{2\pi}{3a_0} \cdot (1, 0)$. Therefore, there are six K points due to the hexagonal form at the first Brillouin zone. In addition, by symmetry, the six K points can be reduced to two independent and inequivalent points: K and K' as it is represented in Figure 2.3 a).

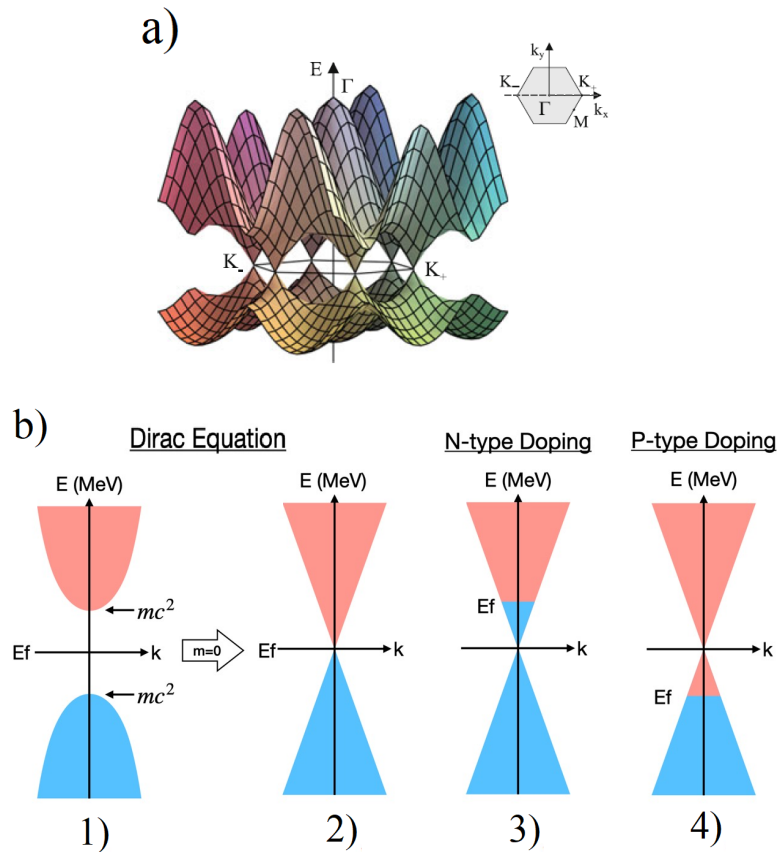


Figure 2.3: a) The representation of the symmetry points and conduction and valence bands at the K points of the hexagonal lattice in reciprocal space. b) From left to the right, 1) it is an approximation of the valence and conduction band at low energy for semiconductors, 2) it is an approximation for graphene that forms two cones touching at Dirac Point, 3) and 4) are for graphene n-type and p-type doping changing its Fermi level¹³.

Those symmetry points are very important in solid state physics field because leads to understand that the valence and conduction band touch each other at those K-points and this only happens for graphene structures which explains electronic properties. In other words, the two bands form two cones touching at the Dirac Point known as Dirac Cone (considering that the system is a low energies for electron transport) as in Fig 2.3 b.2) implies that the bands have a linear dispersion for graphene. Also, the Fermi Level is at the exact point where the bands touch. Due to this touching at Dirac point (not overlapping as for metal materials) and the Fermi level in between, graphene is known as a semiconductor of zero band gap⁸. This is the characteristic feature for graphene because in condensed matter physics, the charge carriers through a material are described by the Schrödinger equation with effective mass or with relativistic description for the particles at the limit of zero rest mass. However, the electrons in graphene have linear dispersion which means that the electrons behave as zero rest mass, relativistic Dirac Fermions.

On Fig 2.3 b.1) is a representation for any semiconductors with a band gap, however for graphene, the representation of the conduction and valence band are linear as cones touching (Dirac Cone)(b2). This gives information about the density of states that increases with energy in linear proportion and also about the electron transport^{8,9}. In addition, if graphene is doped with p or n type as in Fig 2.3 b.3 and b.4, then the Fermi Level will shift and affect directly on the electron transport. It means that due to a controlled functionalization (explained in subsection 2.1.3) with electron donors or electron withdrawing is possible to change the charge carriers transport and the band gap of graphene. In this way, the researchers are focused on surface modification in order to exploit the graphene properties for the fabrication of capacitors, transistor or other devices¹⁰.

In a graphene layer, one carbon atom has three carbon neighbors in the same plane. Due to sp^2 hybridization of carbon atom, it bonds by one of three hybridized orbitals forming a σ bond with the other carbons in the xy plane as is represented in Figure 2.1 a). Those bonds are very strong because have a covalent character. This covalent character allows a more stable and fixed structure. This is the reason why the graphene is a very strong material. Its tensile strength is about 200 times higher than steel¹⁰.

In addition, the 2p orbital (not hybridized orbital) is perpendicular oriented with respect to

the plane. This is known as the $2p_z$ or π orbital and it is responsible for the electronic structure. This orbital influences on the electronic as well as the optical properties because causes that the electrons delocalize in graphene¹². Therefore, the electrons can flow through the π orbitals and the conduction occurs easily. The electrical conductivity of graphene is about 7200 S/m and the thermal conductivity is around 4.8×10^3 W m/K at room temperature. The defects on graphene are produced when the sp^2 structure is broken implying the loss of properties mentioned before⁹.

This knowledge is not enough because for a further controlling of its properties is required its manipulation. The graphene is a very inert material. It means that it does not react with the environment. This causes that graphene can not manipulate as we would desire.

In this subsection was explained the characteristic features for graphene. For the next subsection will be presented carbon nanotubes which is another carbon nanomaterial also used for the purpose of this investigation.

2.1.2 Multiwalled carbon nanotubes

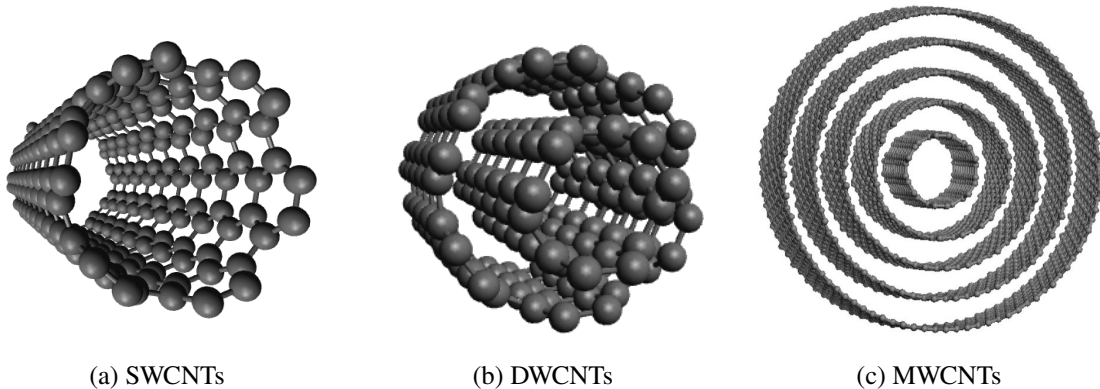


Figure 2.4: Representation of CNTs structures made on Avogadro software. a) is a single-walled carbon nanotube with armchair structure, b) represents to a double-walled carbon nanotube and c) represents a multiwalled carbon nanotube with 5 graphene layers.

Carbon nanotubes (CNTs) are sheets of graphene rolled up, so they form tubes with hollow-

core made from one or more layers of graphene⁷. It means that the structure of carbon nanotubes has carbon atoms with sp^2 hybridization.

The Figure 2.4 has a representation of the classification of CNTs. If the carbon nanotubes are made of one sheet of graphene, they are called single-walled carbon nanotubes (SWCNTs)(Figure 2.4 a). If the nanotubes are made of two layers, they are called double-walled carbon nanotubes (DWCNTs)(Figure 2.4 b). Therefore, if the nanotubes are made of more than two layers, they are called multiwalled carbon nanotubes (MWCNTs)(Figure 2.4 c). For double and multiwalled carbon nanotube, the tube walls are parallel with respect to the tube axis. The tube axis is the direction in which the nanotube grows, making a 1 dimension (1D) material⁷.

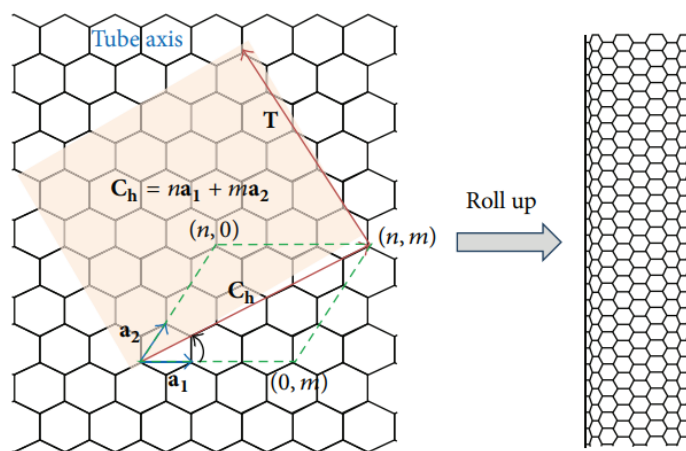


Figure 2.5: Chiral vector which defines the geometrical parameters for CNTs¹.

Some properties as length, direction, diameter and type of edge depend on the rolling vector or the chiral vector (n,m) . As it is represented in Figure 2.5, the chiral vector (C_h) has two indexes: n and m , also the translation vector is T which is the tube axis (perpendicular to the chiral vector)¹. The values of those indexes define the configuration of the nanotube. Based on the chiral vector, it is possible to classify the SWCNTs. If the C_h of a SWCNT is with n equal to m ($n = m$), the nanotubes are armchair tubes type. In the Figure 2.6 a) is an example of the characteristic armchair edge in a nanotube with a $(6, 6)$ configuration. If the C_h of a SWCNT is with m equal

to 0 ($m = 0$), the nanotubes are zig zag tubes type. In the Figure 2.6 b) is an example of the characteristic zigzag edge in a nanotube with a (6, 0) configuration. If the C_h has any other values for n and m , the nanotubes are called simply chiral tubes.

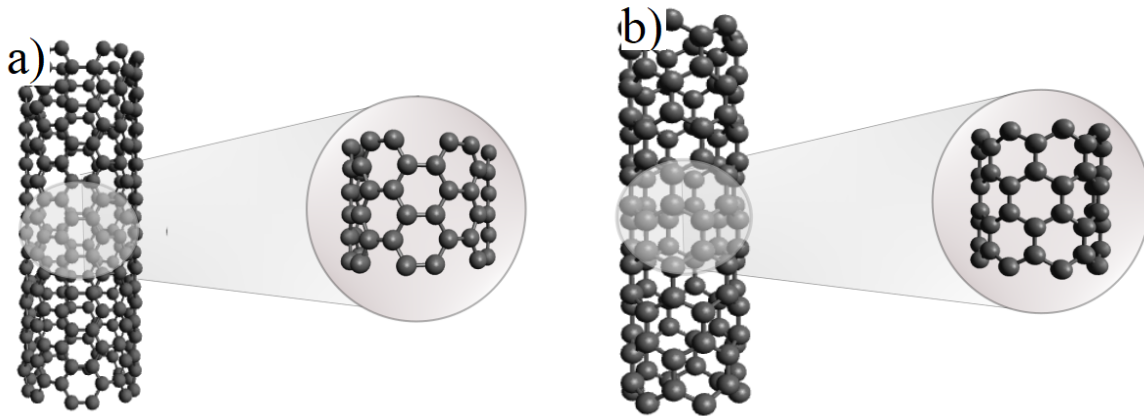


Figure 2.6: a) Armchair nanotube (6,6) b) Zigzag nanotube (6,0). Both nanotubes simulated on Avogadro.

In addition, the chiral vector (values of n and m) defines the electronic properties of the nanotubes because describes how to fold graphene. Some nanotubes result with metallic (when $n-m$ is multiple of 3) or semiconductor behavior and for the MWCNTs are all metallic⁷. This is very important because a metallic CNTs could carry electrical current density until 1000 time greater than a good metal according to the theoretical predictions¹⁴. For this reason, CNTs have caught the attention of researchers and they still continue investigating on this topic.

At the beginning, the first synthesized CNTs were MWCNTs, they were grown on silica substrates with embedded iron nanoparticles. So, the MWCNTs grow perpendicular to the surface but on the iron nanoparticles by forming an aligned array of tubes in a random manner. Since the synthesis process was through CVD, the investigations have been made to control the growth of nanotubes. Nowadays, some parameters as: length, direction, alignment, diameter are controllable with the new synthesis techniques by the use of nanoparticles, glass substrates or catalysts, etc. Ideally, the synthesis method should make the CNTs grow without encapsulation

of contaminants or elements from the synthesis, but it not is always the case and the CNTs need extra process for removing or purification which can damage the structure of the CNTs due to the use of strong acid solutions¹⁵.

In addition, some interesting properties for CNTs are: high tensile strength, high electrical and thermal conductivity, high chemical stability, high ductility and so on. The geometry and structure of the CNTs affect those properties. For example, the Young's modulus of MWCNTs are in the order of several GPa along the tube axis but is softer in the radial (around 1 GPa) direction¹⁴. Also, the electrical properties of MWCNTs demonstrated that the electrical conductivity is much more along the tube axis direction than in the radial axis. This is because of the electron needs to jump from one wall to another when is in radial direction. For instance, at room temperature, the electrical conductivity along the tube axis is 7-14 S/cm while for the radial axis is 1 S/cm. The same happens with the thermal conductivity, CNTs can be good conductors (in tube axis) and insulators (at radius axis) at the same time¹⁴. Finally, given that the carbon forms the same bond as in graphene, the nanotubes are very stable chemically.

2.1.3 Funcionalization of graphene

Before talking about functionalization, it is important to take in mind the next issues¹¹:

- Depending on the synthesis method, the graphene sample might have different size, shape, elemental composition. Therefore, each sample requires a different functionalization process according to the purposes.
- Depending on the synthesis method, the presence of defects on structure can vary. Real graphene always has edges, plane fluctuations, vacancies and impurities. The functionalization process must try to avoid getting worse the structure, otherwise the graphene could not show the desirable properties.
- Due to the very stable σ bonds, graphene has very low chemical reactivity. The bonds are nonpolar covalent, so they are stable and will not react with other species. Graphene is even less reactive than CNTs. Therefore, effective approaches for functionalization are limited in order to not destroy the lattice and to really combine graphene in order to manipulate it.

- Graphene is also insoluble in organic solvents and easy to aggregation in aqueous solution.

Functionalization is a quite wide concept that refers to the modification of materials to give them new functional properties to perform specialized tasks. By attaching chemical functionalities to graphene can improve their solubility and interactions to allow a better manipulation. The functionalization can be: covalent, noncovalent, defect, chemical, etc. However, for this research is important covalent and noncovalent functionalization. Covalent functionalization or chemical functionalization refers to covalent linkage given between the functional entities and the graphene layer. Therefore, the carbon hybridization would change from sp^2 to sp^3 . Noncovalent functionalization or physical functionalization is based on the complexation process and the adsorption forces. Those processes are governed by the Van der Waals and π -stacking effects¹⁶.

Besides, it is important to understand the reactivity of graphene. On the one hand, the covalent functionalization is more likely to happen at the carbon atoms of edges because they usually adopt tetrahedral geometries (sp^3 hybridization) and bond to elements as hydrogen¹¹. Also, zigzag edges as well as vacancies are more reactive sites. Moreover, if there is a curvature at graphene plane, it can produce localized states with higher energies and improve the reactivity¹¹.

On the other hand, the noncovalent functionalization is more desirable and useful because does not destroy the graphene network or change the properties and the main characteristics are kept. For instance, graphene layer can be decorated with transition metals, ions and molecules by complexation reactions or charge transfer adsorption. In this way, graphene would form electron-donating functional groups but does not change the hybridization of carbon nor π bond and electron dispersion. In fact, graphene can be more conductive and improve the transport of carriers through the surface¹¹. So, the functionalization will produce a shift in the Fermi Level to the valence band or conduction band depending on whether the ion or dopant is a donor or acceptor. Moreover, the functionalization could affect the reactivity of graphene becoming into a more processable material which interacts with organic solvents¹⁰. Therefore, this investigation is focused on functionalization between graphene layer with a electron donor and analyze the graphene behavior.

2.2 Characterization Techniques

A new nanomaterial always must be characterized and specially if it has been functionalized in order to verify the change of its properties. There are many different techniques for characterization and each one has different characterization purposes depending on what is the material for. Thus, there are techniques based on the atomic force microscopy (AFM) and scanning tunneling microscopy (STM) which mainly check about the surface morphology of a sample. Other techniques are based on electron microscopy as transmission electron microscopy (TEM) or scanning electron microscopy (SEM) which are used for characterizing morphology, particle size distribution, surface homogeneity and so on. Another techniques use photo-emission spectroscopy as fourier transform infrared spectroscopy (FTIR) which measures the absorption of a light range (infrared) for the identification of unknown molecules in a sample based on the vibrational modes or as Raman spectroscopy which measures the scattered monochromatic light to identify the vibrational frequencies of a structure and identify the defects or quality of sample.

So far, all those technique only can give information about the morphology and physical properties or chemical composition of the samples. Nevertheless, for knowing the functionalization degree of two or more compounds, it is necessary a technique that helps to understand the interaction among atoms. For this reason, it has been chosen the X-ray photoelectron spectroscopy as technique for the characterization.

2.2.1 X-ray Photoelectron Spectroscopy (XPS)

X-ray photoelectron spectroscopy (XPS) is one of the most powerful and precise technique for surface characterization of nanomaterials. This technique provides information about the elemental composition and chemical bonding of a sample. This is a nondestructive technique that has a high elemental sensitivity and gives quantitative information about the surface (around 10 - 200 Å of depth)¹⁷.

Physical principle

The XPS principle is based on the photoelectric effect. In high vacuum conditions, a photon with high energy penetrates a sample surface and interacts with an atom. When it happens the photon

can interact with the electron by transferring its total energy. Also, the photon can pass through the atom without any interaction neither with the electrons nor the nucleus, or the photon can be scattered and lost its energy partially.¹⁷ Nevertheless, the first case of complete transfer of energy is the physical principle of XPS. For this part, it is important to mention that the energy of a photon is:

$$E = h\frac{c}{\lambda} = h\nu \quad (2.3)$$

Where h is the Plank's constant, λ is the wavelength, c is the speed of light and ν is the frequency of the wave.¹⁷ Moreover, it is important to make emphasis that the photon energy comes from X-ray radiation (from 0 eV to 1000 eV) which is a high energy radiation from the electromagnetic spectrum. As it is illustrated in Fig. 2.7 a), the energy of the incident photon is higher in energy than the binding energy of an electron at the core level in the atom, then the electron is excited and ejected from the orbital and the atom called emitted photonelectron. For instance, Figure 2.7 b) is representing the process for carbon atom which is the material of interest.

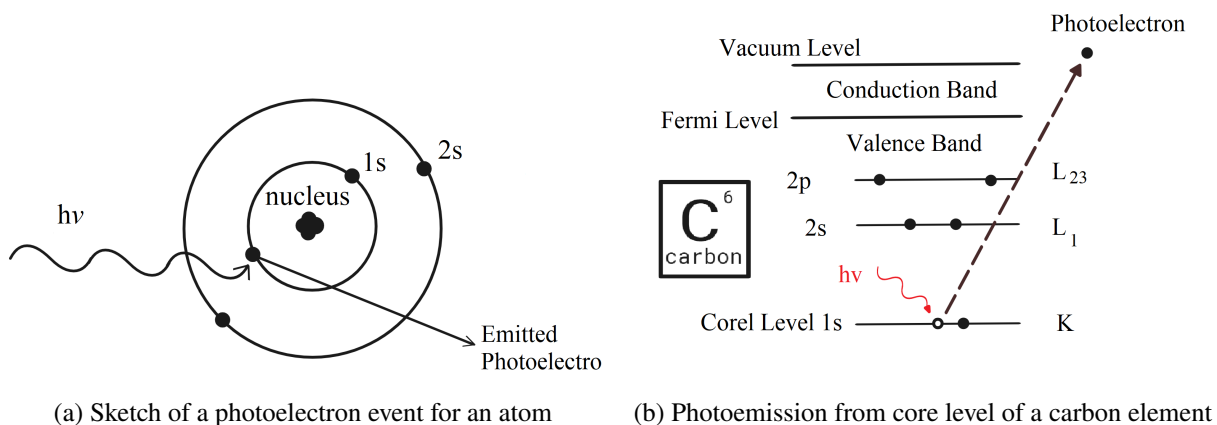


Figure 2.7: Photoelectron process representation.

Hence, the photon hits the electron at 1s orbital and the electron is ejected from the atom with a kinetic energy that is the difference between the photon energy minus the binding energy at core level of the element in the sample. Thus, it is possible to know the binding energy of the

ejected electron by:

$$E_b = h\nu - E_k \quad (2.4)$$

where $h\nu$ is the photon energy (with ν in X-ray frequency), E_k is the kinetic energy measured by the equipment and the E_b is the binding energy for the atom from 1s orbital.¹⁷ Binding energy differs from species to species and is at specific ranges for each element of the periodic table. Therefore, with this technique is possible to identify the elemental composition presented in a sample. The binding energy is normally expressed in electron volts (eV).

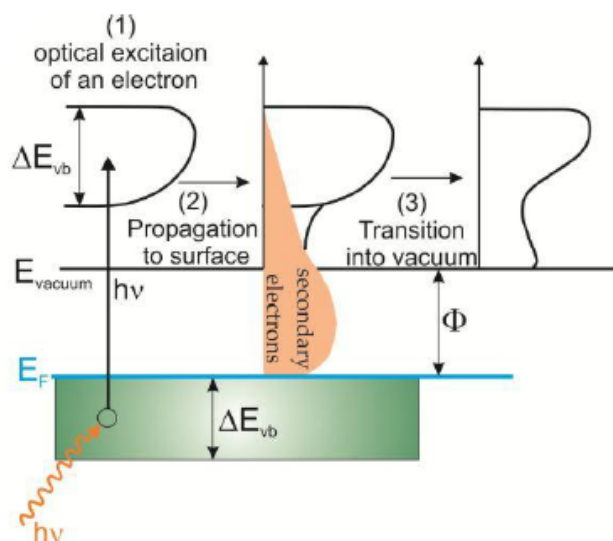


Figure 2.8: The schematic representation of the photoelectron process. This is the three step model explaining the optical excitation, propagation through the surface and transition of electrons into the vacuum¹².

There is a three step model that allows a better description of the photoemission process¹². The model is explained in Figure 2.8. The first step is about the optical excitation (Fig Figure 2.8.1). A X-ray radiation crosses the high vacuum until reaches the surface sample where the electron is excited from its initial state (at the core level) for the incident photon. The second step is about propagation through the surface (Fig Figure 2.8.2). The excited electron is ejected and does not belong to the atom anymore, so can travel through the surface sample. The propagation

is given by mean free path and it only depends on electron-electron or electron-phonon inelastic interactions because any other type of interaction is not considered given that the system is in high vacuum. Whether these interactions are presented, then they will contribute to the background of the spectrum (the result of the measurement). This is the reason because of this technique is for surface characterization, otherwise the electrons generated at bulk will not be capable to travel large distances until the surface and then toward the vacuum.¹⁷ Finally, the third step is about the transition into the vacuum (Fig Figure 2.8.3). Due to the system is at high vacuum, the electron needs to pass through the surface sample and must overcome the work function Φ of the sample itself to enter the vacuum toward the analyzer and detector (which are responsible for measuring the electron emitted)¹². At this point, equation 2.4 was a first approximation but it is not considering neither the work function of the sample Φ_s nor the work function of the analyzer Φ_a (part of the equipment).¹² Therefore, the equation is rewrote as follows:

$$E_b = h\nu - E_k - \Phi_a \quad (2.5)$$

Furthermore, some parameters as: the lattices parameters, the symmetry breaking and the electronic dispersion direction would influence on the three steps. The result after the characterization is a spectrum of emitted photoelectron intensity as function of the binding energies¹⁷. Therefore, each excited atom is presented at an specific range of energy and represented by a peak intensity in a spectrum that allows to identify a specific element by using already reported data of pure or functionalized materials.

XPS is a standard method to explore the chemical environment and composition of a surface because of the initial and final states of the electron excitation strongly depends on the many-body interactions in the sample and the relaxation process of the hole state. Therefore, the binding energy (E_b) is related to the binding energy of each atom (E_b^{atom}) plus the energy of the chemical surroundings (E^{chem}) per atom and the relaxation energy (E^{relax}) coming from the many-body interaction and the relaxation process due to the hole produced¹².

$$E_b \sim E_b^{atom} + \delta E^{chem} + \delta E^{relax} \quad (2.6)$$

The XPS technique is sensible to chemical changes because although the excited electrons are from core level, they are also influenced by the electrons from the valence and conduction

bands. Therefore, the presence of doping materials or functionalized materials will be observed as shift in binding energy of the center of the peak at the spectrum¹². For example an oxidized surface, the electrons of valence band (from the oxidized element) will be donated to the oxygen atom and the core electrons are more difficult to eject due to increased coulombic interaction. Therefore, the signal for an oxide case is at higher binding energy compared to a pure one (not oxidized one). When the surface is a more complex system by multiple materials, then there will be some shift due to the chemical environment. The reason is because of the binding energies are strongly depended on the electronegativity changes at the structure of the sample and the chemical bonding on surface¹².

Experimental set-up for XPS

In general, XPS measurements are carried out over a the sample which is placed in a sample holder, both are inside of a chamber in high vacuum or ultra high vacuum conditions (from 10^{-9} mbar). Inside the chamber, there are: an electron gun, anode, monochromator, sample holder, hemispherical analyzer and detector as in Figure 2.9 is represented.

The process starts at the electron gun. A filament is heated and produces electrons which are accelerated by a potential difference (about 20 kV). The electrons hit the anode with high energy and produces some photons at the X-rays range by the recombination process. Then, only the high energy ones interacts with the monochromator which selects the X-ray radiation passes through it. The X-ray radiation comes generally of aluminium or magnesium because those materials provide stable and reliable beams of $K\alpha$ X-ray coming from $K\alpha_{1,2}$ transitions¹⁷. In this way, the monochromator allows the use of stable signal with same range of wavelength for the measurements. Then, the X-rays crosses through the vacuum towards to the sample. After the photoelectron process, the emitted electrons from the sample pass through the vacuum and enter to a energy dispersed element, hemispherical analyzer. So, the hemispherical analyzer causes a deceleration and deflection on the electrons. Only those electrons with high energy (coming from core level) are able to be focused on outer sphere, the rest of the slower electrons got lost inside the sphere. At the end, the electrons reach a electron multiplier detector and the resulting pulse of electrons goes to a small multichannel plates that generates a photon signal detected by a CCD camera.^{12,17}

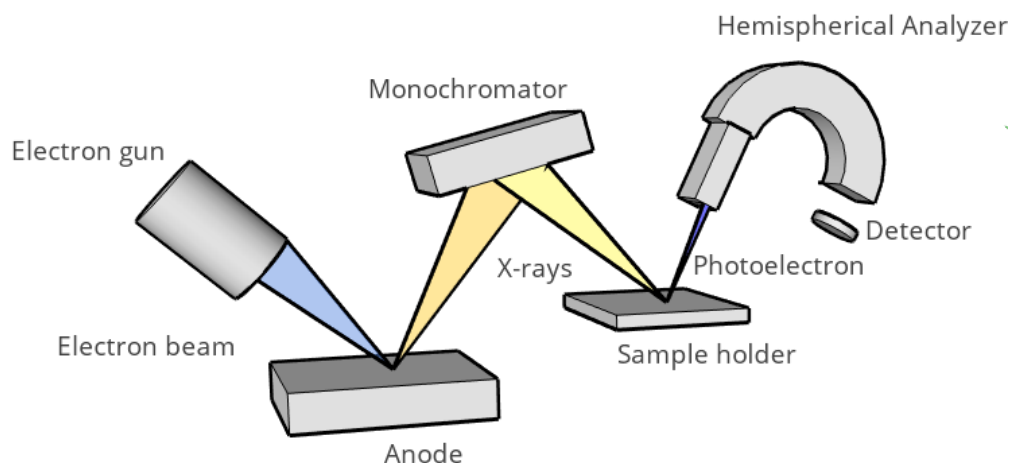


Figure 2.9: Schematic representation of XPS system with the principal components for the measurement.

XPS data interpretation

When characterization finishes, an spectrum with binding energy as x axis and number of electrons detected (intensity) as y axis is presented at the screen of the software of the equipment. First, the equipment always does a scanning from low energies (around 0 eV) until high energies (more than 1300 eV) with a high step energy to analyze briefly the sample at low spectral resolution called survey spectrum^{17,18}. The survey spectrum helps to identify where are the regions with high intensities that present peaks which means the presence of elements. Next, once the energy range is identified a new scanning on that defined region is performed with a lower step energy for obtaining higher resolution spectrum, it is the narrow spectrum corresponding to an specific element to analyze the bonds and type of interactions. There can exist several type of peaks depending on the physical or chemical origin on a high resolution spectrum¹⁸.

It is very important to understand the origin of those peaks. The principal peaks or lines are independent each other and they can be¹⁸:

1. *Photoelectron Lines*.- those are the most intense lines produced and with narrow shape in survey spectrum. In the narrow spectrum from a specific region, the width of the peak is the result of convoluted peaks. The width of each peaks is related to the life-time of electron until is recombined. It is know as full-width half maximum (FWHM). Those lines are the main peak which gives information of the elemental composition of a sample based on the binding energy to which is.
2. *Auger Lines*.- those lines are produced for auger process which happens when the an electron recombines and releases enough energy to eject another electron from the last orbital. So, the lines appear independently from the ionization energy.¹⁸ Those line are presented in complex patterns and are related to vacancies on the structure.
3. *X-ray Satellites*.- those lines are related to mirror peaks that happen at lower binding energies caused by higher photon energies and the use of a monochromator.
4. *X-ray Ghost Lines*.- those lines are produced for X-ray radiation coming from an element of the sample material, instruments or contamination. The lines are weak in intense and very uncommon to appear.
5. *Shake-Up Lines*.- those lines are related to ions that were left in an excited state instead of coming back to the ground state. Those peaks usually appear a few electron volts displaced in binding energy from the main peak.

In addition, in order to avoid a positive charge at the sample surface is used an electron neutralizer or the samples must be placed on a conductive surface. Each of those lines are independent from each other and they are present at different places in the spectrum. Given the description of those lines, it is clear that from a measured XPS spectrum, there are two type of information. The primary information is related to the photoelectron lines and auger electrons which are the principal information about the chemical composition, concentration and electronic properties of the sample. They are registered in the survey scan or the region scanning. The photoelectron lines are also presented and recorded in the high resolution scans (by the specific regions)¹⁹. The secondary information are related to the complementary information as background or the rest of lines that are not related to photoemission¹².

For the narrow spectrum or region spectrum or high resolution spectrum, it is important to clarify that due to the presence of many components from a sample and for extracting the values characteristics from the peaks is necessary mathematical functions to recreate and obtain or fit the intensity, binding energy, width, etc from the obtained spectrums for regions. A good fitting or a good approximation to the spectrum can be achieved by using Shirley or Tougaard backgrounds and Gaussian-Lorentzian curves for main peaks¹⁹. If in the sample exists more than one allotrope for a specie, then there will exist a peak per allotrope (if the concentration is enough). So, the peaks will be very close in binding energy because are from the same element. So, any spectrum from XPS characterization is always the result from a convolution of peaks. Convolution is a mathematical operation of two or more peaks that produces a global peak expressing the shape of one modified by the others²⁰. Therefore, it is very common that the spectrum requires a deconvolution, which is the opposite process of convolution, to obtain the individual peaks. This means that the main peaks of a spectrum (focused on a region) can be deconvoluted into two or more peaks which must be assigned using reported data parameters to avoid errors²⁰. Only for pure samples have sharp peaks, for combined elements are wider peaks. The finding of better functions with the best suitable parameters, deconvolution peaks and so on is known as peak fitting which leads to a spectra analysis¹⁹. Nevertheless, it is always important to first understand the chemistry behind before entering the number of peaks that might be involved at the deconvolution process as a first guessing. Otherwise, it could be a lost of time to enter information of elements that do not belong to the sample.

Thus, the first step at the data treatment of a spectrum in a software is to find a suitable background. It influences on the main characteristics of the next steps. The used algorithms for this investigation were: Shirley and Tougaard backgrounds. Shirley background is assumed that the background intensity increases at higher binding energies because the inelastic scattering of electrons at the peak center energy also increase. This causes a smooth step like function¹². The Tougaard background is based on the probability that an electron could undergoes an ineffective energy transfer and appears at the background. The second step is, the use of Gaussian-Lorentzian or Voigt functions for the lines shapes²⁰. With those functions, the data is localized to the position of the peak in a symmetry manner. Depending on the material Voigt functions are normally used for any material unless it is a metallic material. Metallic material presents asymmetric peaks and

it is required Doniach-Sunjic functions which are used for asymmetric peak behavior¹⁹. All those functions are already in the software, the researcher has to use reported data parameters from XPS measurements as binding energy and FWHM appropriate to the experiment. If the parameters are correct for the analyzed compounds, the software will generate a fitting good enough to obtain simulated spectrum, which must be very similar or very close to the real measured spectrum. Only when the spectra (real and simulated) are similar, then the parameters used for the fitting are the true information about peaks of the spectrum that comes from the sample characterization. That information tells about the nature of the elements, the type of bonds, the functional groups present and so on.

2.2.2 XPS in graphene and multiwalled carbon nanotubes

For the carbon materials, if the material is pure, then a XPS survey must present a high intensive peak related to only carbon and the rest of the spectrum must be flattened. If there is a presence of other element, then will also appear. Besides, the XPS high resolution spectrum is focused on the C1s region which is for carbon. In C1s region, the presence of different carbon allotropes will affect the main peak, its shape and the binding energy and will be all present at this region. It means that if variants of carbon (even bonded with other elements) species coexist in the sample surface, they will be revealed at C1s region¹⁹. For graphene and CNTs, the C1s peak typically appears around 284.45 eV^{18,21}. In Figure 2.10 is shown a survey spectrum for a carbon material with oxygen. The survey presents a very intense peak corresponding to the presence of carbon around 284 eV and oxygen around 531 eV¹⁸. The rest of the spectrum is flat which means that there is not any other element. At the narrow spectrum or spectrum for region, is shown the C1s region with a peak centered to ~284.5 eV and with a width of just one peak due to the purity of the material. Also, the Fig. 2.10 shows the importance of a monochromatic source because the spectrum is broader without it (red line) and it could lead to a mistake at the analysis¹⁹.

In graphene and CNTs, the shape of the main peak (centered a 284.5 eV) at C1s region is related to the density of state near to the Fermi edge. The Fermi level is very low and causes that the electron-hole pairs are easily created and influences on a parameter as the full width half maximum (FWHM) which is related to the lifetime of the electron recombination after the ejection for the electron from the core level. While the peak centered at 284 eV becomes wider,

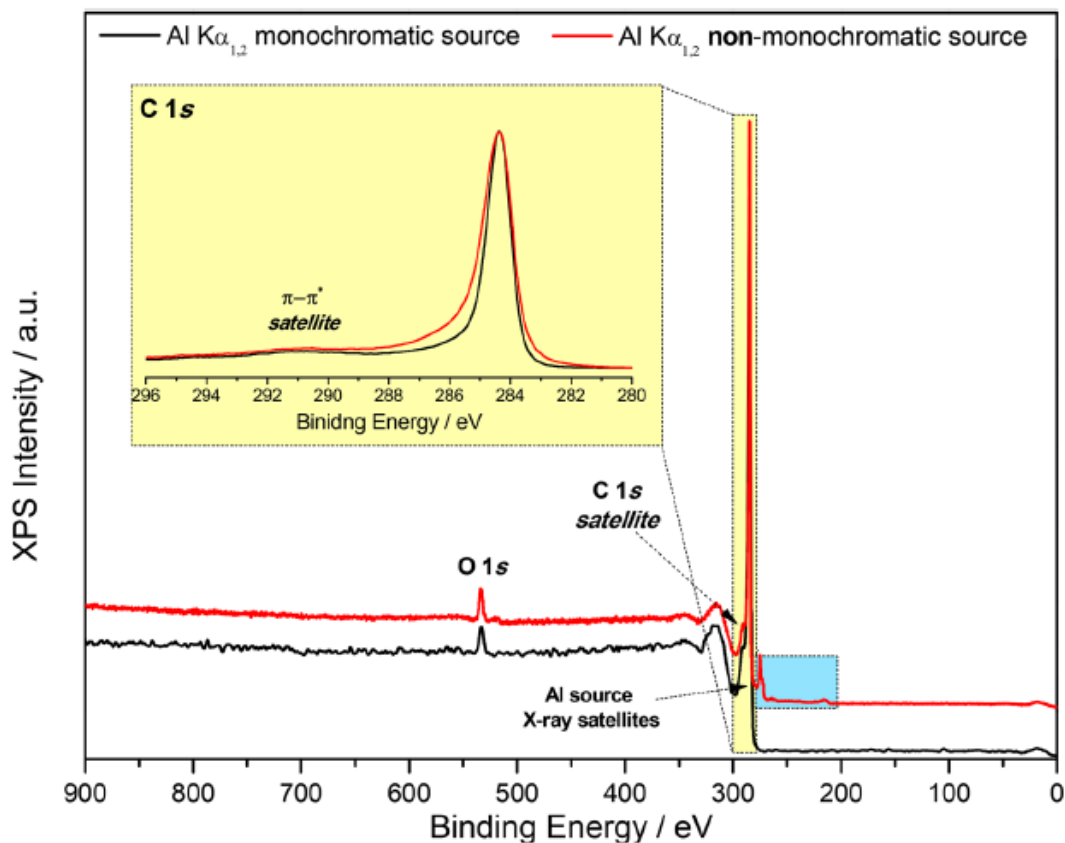


Figure 2.10: Survey and high-resolution spectra of a graphite sample recorded by a monochromatic and non-monochromatic $\text{AlK}\alpha$ X-ray source¹⁹

then assumption of the presence of defective sites or functional groups is more accurate in carbon structure. Also, the peak intensity is related to the amount of the element on the sample, then it is possible to analyze the chemical bonding of an element based on the predominant peak in the region¹⁹. In this way, it is possible to know the quality of the carbon material. For instance, at C1s the peak for sp^2 hybridization is usually at 284,5 eV but for sp^3 hybridization is at one eV higher²¹. Then, depending on which peak has the major contribution on the C1s region, then it is possible to state if the sample is amorphous or ordered material¹⁹.

Many investigations are focused on the graphene and the properties modification²². In fact, doping graphene layer with alkali metals has been a topic of intense research because the metal can act as an electron donor and the graphene can act as an electron acceptor²³. Then, potassium is one of the common dopants for surface modification, this method is used to adjust the electronic properties for graphene. In this way, graphene can become into a n-type-doped semiconductor enriching its electronic conductivity²⁴. By the characterization techniques as cyclic voltametry can confirm that the potassium acts as an electron transfer to promote the charge transfer at graphene surface. According to Xiao-Rong Li et al., the potassium-modified graphene is highly sensitive and stable for electrocatalytic activity, also it can be used as a sensor due to the improved detection limit²².

However, by XPS characterization is possible to establish how affects the potassium to the carbon network. If potassium contributes to charge transfer or modifies the carbon hybridization only can be described by the XPS measurement where the position of the peaks reveal about the type of bonds and the shape of the peaks demonstrating information about the atomic interactions. For instance, a XPS analysis from the core level spectrum of potassium-doped graphene shows the presence of the alkali metal in the C1s region confirming the deposition of the metal on graphene surface²⁵.

Chapter 3

Motivation and Research objectives

Based on the presented background, it is clear that graphene and MWCNTs are interesting materials due to their physical properties and the possible technological applications. For graphene, many investigations have been focused on: controlling its properties by a doping process with alkali metals in order to avoid destroying the graphene structure and improve the charge transport by giving it a donor dopant whose electrons will contribute with the electronic dispersion²² and also about changing its properties with functionalization with functional groups to become it into a more reactive material¹⁰.

However, a graphene functionalized with potassium and functional groups can become it into a novel material, more reactive, with better electronic structure or less hydrophobic behavior and available for technological applications as for electronic devices or biochemical sensors. Thus, the purpose of the investigation is to analyze such material through XPS. The behavior of this functionalized graphene can be tested in different environments to understand how was the degree of functionalization and chemical interactions.

At the same time for MWCNTs, the synthesis method defines the quality and the main features of the material. Moreover, the purpose of this investigation is also a XPS characterization of the MWCNTs synthesized for first time in Yachay Tech University and in Ecuador to confirm the quality of the material that should be pure and could be used as a reference given that it has not been subjected to any functionalization process or surface modification.

The general objectives are:

- Analyze the XPS spectra for potassium-doped graphene to understand the functionalization with the dopant and functional groups after the different types of functionalization environments to comprehend the chemical interaction at the graphene surface.
- Analyze the XPS spectra for multiwalled carbon nanotubes in order to confirm the quality of a material and its properties given that the material can be used as a reference for non pure materials because it has not been functionalized.

Therefore, the main specific objectives for this thesis are:

- Prepare of potassium-doped graphene and MWCNTs samples.
- Characterize by XPS the graphene and MWCNTs samples which implies the survey and high resolution measurements.
- Determine the chemical composition and atomic percentages for the graphene and MWCNTs samples using the information on survey spectra .
- Determine the functionalization or purity of the graphene and MWCNTs samples using the information on the high resolution spectra of the C1s and O1s region.
- Determine the properties and the changes found on graphene and MWCNTs samples.

Chapter 4

Methodology

In this chapter, the synthesis methods and experimental information are presented as well as the fitting process used. The first part is about the transfer process for graphene on a gold substrate, the process for doping it with potassium and also about the different environments to which the graphene samples were exposed. The second part is about the MWCNTs synthesis process. The third part is about XPS details and relevant information used for the characterization of the samples for both graphene and for MWCNTs. The fourth part is fitting process, deconvolution of peaks and peak assignment based on the spectra for each one of the different samples.

4.1 Synthesis of functionalized graphene samples

The graphene samples passed through three different process. The details are presented in three main parts with the aim of understanding the possible interactions at the sample that could be found at the characterization measurements. In Figure 4.1, there is a sketch summarizing the next description.

- **Transferring process for graphene**

A CVD-grown monolayer graphene was transferred on gold (Au) substrate or wafer. In order to do this, the Au wafer was pre-cleaned by washing with pure acetone to remove contaminants. Next, Trivial Transfer Graphene from ACS Material (commercial sample) was covered with polymethylmethacrylate (PMMA) for the transfer process (Fig 4.1 b).

The layer of PMMA was expanded by spin-coating onto the graphene layer.

The PMMA is a homogeneous, amorphous, and dielectric polymer²⁶. The polymer acts as a support of graphene to remove it from the previous substrate and place it to new one: Au wafer which is a more conductive surface suitable for the XPS measurements. The chemical composition is $(C_6H_{10}O_2)_n$ ²⁶. The polymer has many oxygens in carboxyl and carbonyl groups at the PMMA structure.

Then, the graphene with the coated film of PMMA was released into bidistilled water to remove the polymer and deposited the graphene-PMMA onto the Au wafer. It means that PMMA layer stayed in the top layer, the graphene in the middle and the Au wafer at the bottom layer (Fig 4.1 c)). Next, it was naturally dried in the fume hood for 30 minutes (room conditions). To remove the PMMA layer, it was used a round bottom flask in which was filled with some acetone. After, the graphene wafer was placed with the help of tweezers into this flask but without touching the acetone. The acetone was heated to 50 °C and its steam removed the PMMA layer since this polymer can be dissolved in acetone. The sample was steamed in an acetone bath for 90 minutes. Afterwards, the graphene layer was baked on the gold wafer at 100°C for 20 minutes using a heating plate. The result was a graphene layer over Au wafer as in Fig 4.1 d).

- **Potassium doping for graphene layers**

The doping process was performed for graphene samples already placed on Au substrate. So, a cleaned glass ampule was sealed under high vacuum conditions ($10^{-6}mbar$). Previously, on the one side of ampule was placed the Au wafer with graphene and on the other side potassium sample (99.95% purity, from Sigma Aldrich) as it is represented in Figure 4.1. Then, the potassium side was heated for 9 hours and 50 minutes at 125 °C, it causes that the potassium ions were heading towards to graphene-gold wafer by a temperature gradient. At the end, the residues of potassium on the sample were removed by heating the wafer overnight at 100 °C.

- **Functionalization process for potassium-doped graphene samples**

After the doping process, the glass ampules were opened in a glove box (with concentration of O₂ and H₂O less than 0.1 ppm) and the samples were functionalized in different environments. One potassium-doped graphene sample was exposed to air (just O₂), other potassium-doped graphene sample was exposed to water (drop of distilled water), other potassium-doped graphene sample was covered completely with two drops of hexyliodide (CH₃(CH₂)₅I from Sigma Aldrich, commercial sample) in the glovebox under argon atmosphere and the reaction time was 40 minute. The excess of the reagent was removed using a tissue paper. At the end of all the process, the respective gold wafer samples were brought out and were stored under ambient conditions.

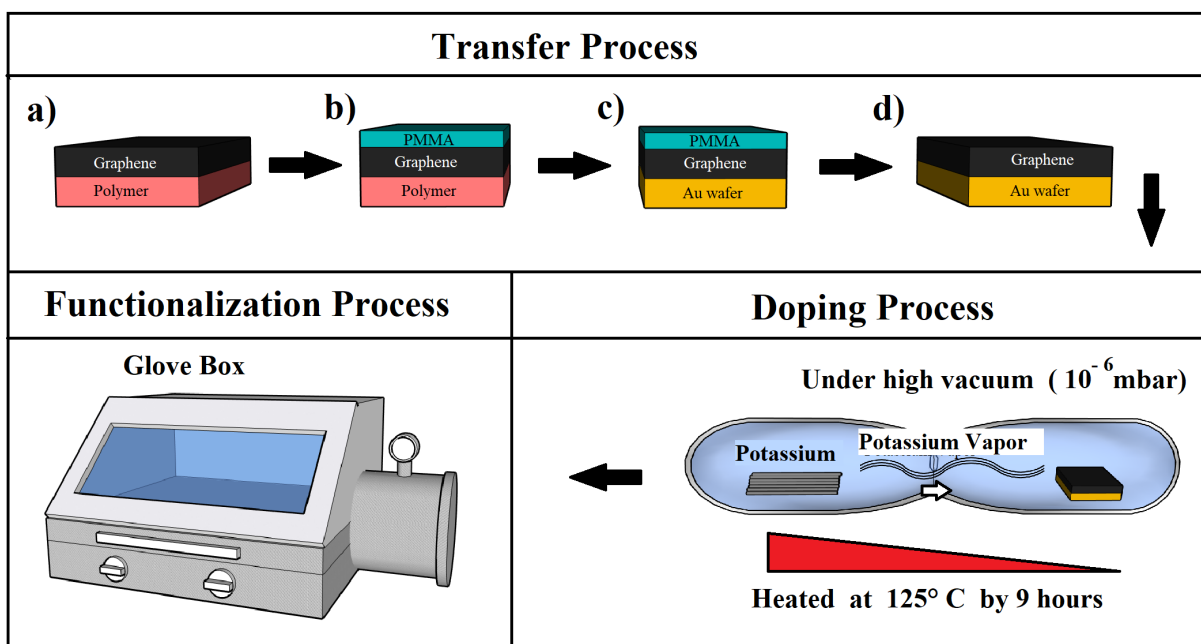


Figure 4.1: Synthesis processes for graphene samples

Finally, there are four sample to analyze with XPS technique. The first sample is the graphene layer transferred to Au wafer considered as graphene pristine (Gr). The second sample is the potassium-doped graphene layer on Au wafer exposed to air (K@Gr+O₂). The third sample is the potassium-doped graphene layer on Au wafer exposed to water

(K@Gr+H₂O). The fourth sample is the potassium-doped graphene layer on Au wafer exposed to hexyliodide (K@Gr+Hex).

4.2 Synthesis of CVD multiwalled carbon nanotubes

The multiwalled carbon nanotubes were elaborated at Yachay Tech's laboratory. The synthesis method was CVD with a carbon source of acetylene (C₂H₂). The MWCNTs were synthesized by catalytic decomposition of acetylene. For the process was used iron (Fe) and cobalt (Co) catalysts supported on calcium carbonate (CaCO₃). The whole process was carried out at 750 °C. So, it was introduced 50 mg of catalysts (previously mentioned) and a 280 mL/h argon flow. Once, the system temperature was at 750 °C, a 120 mL/h acetylene flow passed through the system during 15 minutes. Finally, after the 15 minutes, the source of C₂H₂ was stopped and the system was allowed to cool down until room temperature in presence of an argon flow of 50 mL/h. In Figure 4.2 is a representation of the synthesis method.

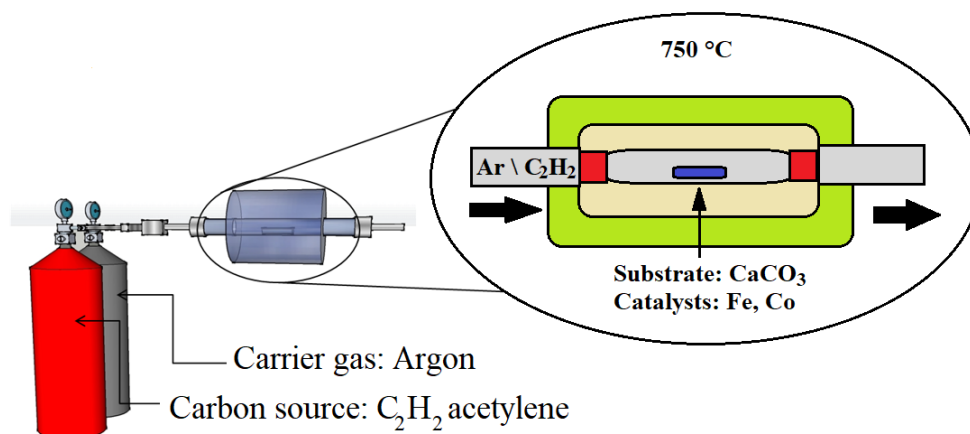


Figure 4.2: Synthesis process for MWCNTs. Sketch adapted².

4.3 XPS measurements

There are some information about the characterization process which will be described below.



Figure 4.3: XPS equipment at MONS University used for measuring graphene samples.

For the graphene samples, the XPS measurements were performed in a VERSAPROBE PHI 5000 from Physical Electronics at MONS University in Belgium. For X-ray source, the equipment has a monochromatic aluminum K_{α} as a source. During the measurement, the analyzer was disposed at 45° with respect to the surface of the sample holder. The power of the X-ray was about 47.6 W. Also, the beam diameter for the x-ray was $200 \mu\text{m}$. For the used energy, the pass energy for analysis of the individual core level region was 23.5 eV and the energy resolution was 0.6 eV. In addition, for the compensation of built up charge on the sample surface during the measurements a dual beam charge neutralization composed of an electron gun (~ 1 eV) and an argon ion gun (≤ 10 eV) was used. The equipment is presented in Figure 4.3.

For the MWCNTs, The XPS measurements were also performed in a VERSAPROBE PHI



Figure 4.4: XPS equipment at Yachay Tech University used for measuring MWCNTs samples.

5000 from Physical Electronics at Yachay Tech University in Ecuador. The equipment has a monochromatic source of aluminium K_{α} for the X-ray source. The analyzer angle with respect to the surface of the sample was about 90° for a maximum penetration of the beam (about 7 nm approximately). During the experiment, the spot size was $100 \mu\text{m}$. Besides, the pass energy for the survey was 250 eV, the pass energy for the individual core level region was 55 eV and the energy resolution is about the 0.5 eV. Finally, it is used a electron gun and an argon ion gun for the charge neutralization. The equipment is presented in Figure 4.4.

4.4 Fitting Methodology

For the fitting procedure was used the next two software: MultiPak and Origin Pro.

MultiPak version 9.8.0.19 is a data analysis software for photoelectron spectrometry and Auger electron spectroscopy. For this investigation, this software was used for exporting the file coming from the XPS equipment into files in txt format to use in Origin Pro. Only this program can open the generated files from the measurement and can reduce the data according to the objectives. In this case, the required data is the survey spectra (for all the samples) and the high resolution spectrum for specific regions as: C1s and O1s for graphene samples and for MWCNTs. Also, the software provides information about the atomic percentages of the elements

on the sample surface. This information is used for the elemental analysis.

Origin Pro 2018 is a software used for the fitting of high resolution spectrum. The software has a tool called Peak Analyzer which is mainly focused for the analysis of background and convoluted peaks in narrow spectrum. This software is used for the fitting of C1s region and O1s region as graphene samples as MWCNTs.

4.4.1 Calibration of a XPS spectra

The calibration is to adjust the spectrum to the right values using a measurement reference due to a previous charged surface not related to the chemical environment of the sample. This is important because if some carbon allotropes are insulators, then they have a positive charged surface due to the photoelectron emission causing a shift in binding energy but it is not related to their chemical state, only due to electrostatic charging¹⁹. Then, all the spectra need to be calibrated or adjusted to the right values in order to avoid a bad peak assignment. So, before the measurement of samples is carried out, it is measured a standard material with a well reported binding energy as a reference to shift the spectra until the reported binding energies of the material.

For the calibration of samples, it was used gold (Au) as a standard reference because is a metal conductor and it is less likely to occur a shift by charging surface¹⁷. Thus, Au 4f is the reference used because presents two peaks are well reported. The first peak is at 84 eV and the second at 88 eV corresponding to $4f_{5/2}$ and $4f_{7/2}$ respectively¹⁸. In the Figure 4.5 is possible to appreciate the calibration for the Au 4f of the potassium-doped graphene measurement. The red line is the spectrum without the calibration and the black line is the spectrum calibrated with the corresponding shift to the reported values for Au4f.

The raw data coming from the experiment was plotted at Origin Pro obtaining a spectrum (red line) for Au 4f but the peaks are not centered at the reported values. Therefore, whenever the peaks are, they must be shifted until their right positions (centered peaks at 84 eV and 88 eV).¹⁸ The added or subtracted value is the constant to be added for all the spectra of the samples measured with this Au 4f reference. In this way, that constant is the calibration for all the data. For the case of Figure 4.5, the whole spectrum is shifted 5 eV towards to higher binding energies.

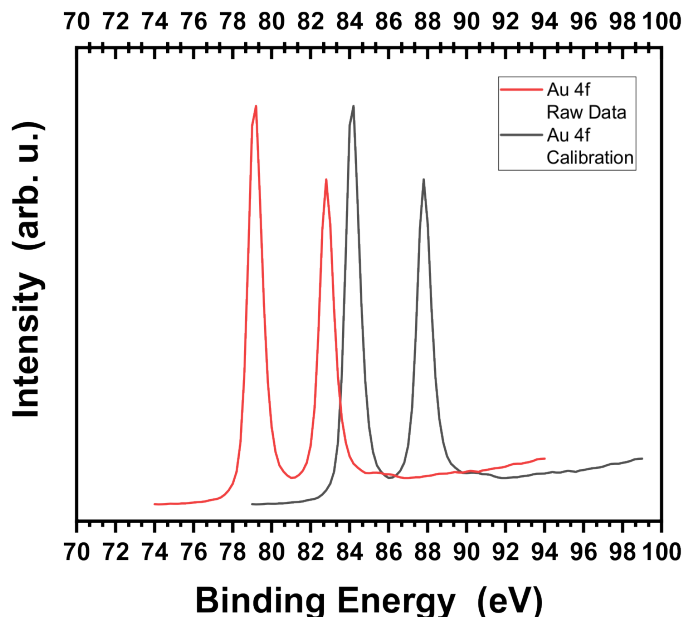


Figure 4.5: Au 4f spectrum. The red line is the original spectrum coming from the raw data. The black line represents the spectrum calibrated with the peaks centered at the 84 and 88 eV¹⁸

The calibration for each sample was performed by using the Au4f_pristine, Au4f_air, Au4f_water and Au4f_hex spectra respectively in order to obtain the right values for each measurement. In this way, the calibration suggested to add 5 eV for Gr sample, 4.2 eV for K@Gr+O₂ sample, 4.6 eV for K@Gr+H₂O sample and 4.8 eV for K@Gr+Hex sample. For MWCNTs, the data was already well calibrated.

4.4.2 Peak deconvolution

The peak deconvolution process is detailed below and was realized for C1s region from 280 to 300 eV and O1s from 526 to 538 eV region spectra obtained for all the samples in Origin Pro. In addition, this process was realized after the corresponding calibration for each sample. The txt file is opened in Origin Pro in a new workbook. From the four columns of data (kinetic energy, binding energy (BE), counts per second (CPS) and background), the BE is set as x axes and the

CPS or intensity is set as y axis. Then, the specific value of the calibration is added to BE. The value is a different one for each environment. Next, the two columns of x and y axis are selected in order to use the tool Peak Analyzer. Peak Analyzer is a tool from Origin Pro specialized for fitting of XPS spectra analysis. After that, the parameters are set as: baseline mode XPS, Tougaard baseline as background, energy range (depending on each sample), not subtraction of information from the background (to avoid losing information) and assigning the number of convoluted peaks.

At this point, a window with information about the peaks is opened to modify the parameters in order to get a good fitting. The Voigt functions were used for all the peaks from elements as carbon and oxygen except for a peak of MWCNTs, it was used Doniach Sunjic function. For each peak had 4 parameters to be modified as: center of peak, area, Gaussian contribution (FWHM) and Lorentzian contribution. The parameters as center of peak (in eV at binding energy) and full-width half maximum (FWHM) are introduced according to the reported data per each spectrum that was deconvoluted. Only when the R^2 parameter (statistical measure of how close the fitting is to data) is closed to 1 or closed enough, it is possible to say the fitting is a good approximation because the plot from the data and the fitting are almost the same. It means that the peaks are well assigned and the information of the peaks are valid for the spectrum from the experiment performed. The average value of R^2 for all the spectra of C1s and O1s regions is 0.951, which means that the fitting are accurate approximations to the data obtained. (For more details see Section Appendix A)

Chapter 5

Results & Discussion

For this section, the results and discussions are focused firstly for graphene samples and later for MWCNTs samples. For both cases, it is presented the elemental analysis using the survey spectra and the atomic percentages and then the high resolution analysis for C1s and O1s regions from each sample in order to obtain the deconvolution of peaks and assign functional groups based on binding energies of possible interactions between elements in the corresponding environment.

5.1 Graphene samples

5.1.1 Elemental analysis of graphene samples

In Figure 5.1 is presented the surveys spectra for the four graphene samples. From the bottom to the top of the Figure the surveys belong to: a) graphene (Gr), b) potassium-doped graphene exposed to air (K@Gr+O_2), c) potassium-doped graphene exposed to water ($\text{K@Gr+H}_2\text{O}$) and d) potassium-doped graphene exposed to hexyliodide molecules (K@Gr+hex) samples. In general, the four surveys show main photoelectron lines related to an elemental composition of: carbon, oxygen and gold which correspond to the graphene material, a possible oxidation process of graphene and the Au wafer respectively. For the doped samples, the surveys show the presence of potassium peak coming from the superficial deposition of potassium except for K@Gr+Hex sample which is explained in the high resolution analysis (See Subsection 5.1.5). This potassium photoelectron line is an evidence of the potassium ions deposited on the graphene surface coming

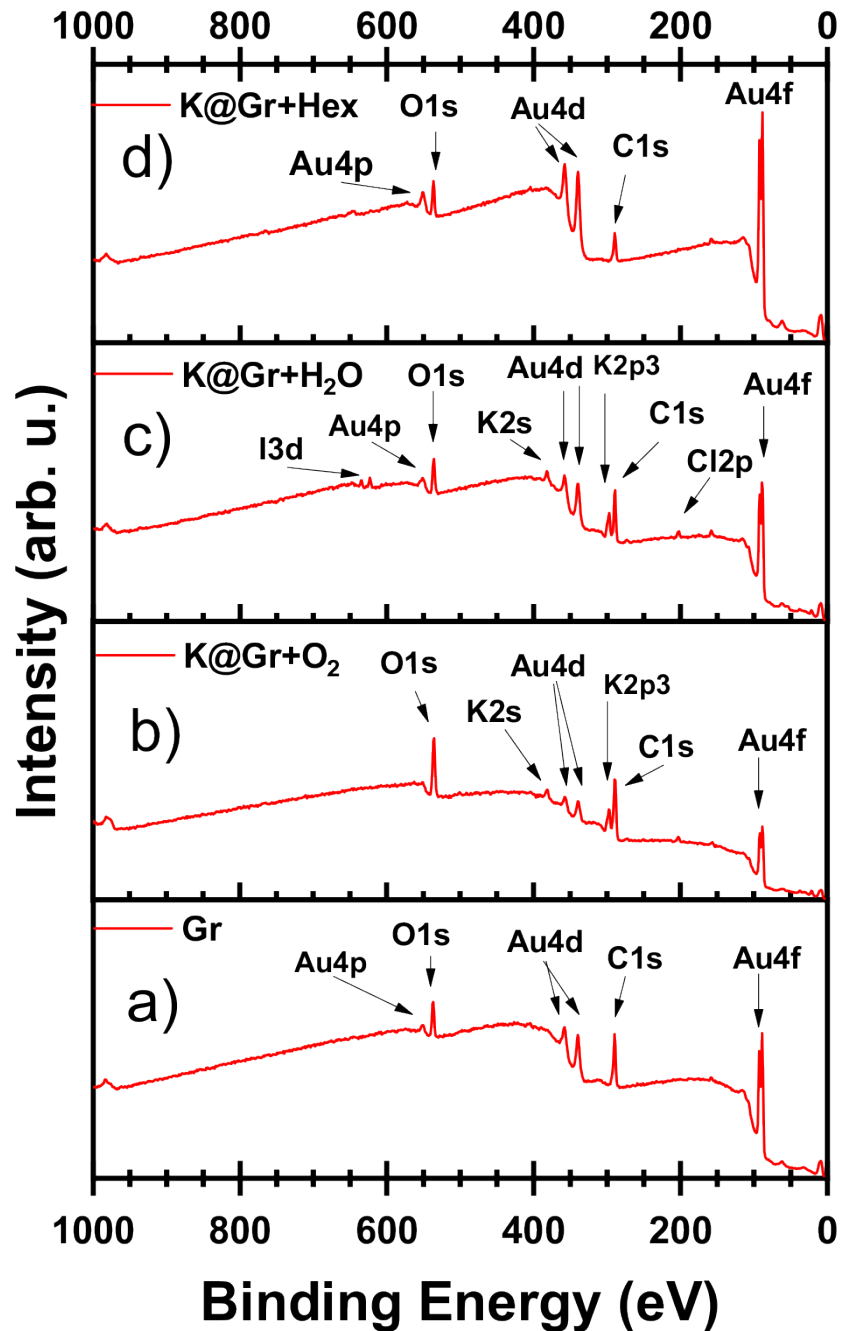


Figure 5.1: Measurement of XPS spectra surveys of: a) Gr, b) K@Gr+O₂, c) K@Gr+H₂O and d) K@Gr+hex samples. The measurements of these samples were made in a range of energy from 0 to 1000 eV.

from the synthesis process, otherwise the potassium peak would not appear at the survey spectra as it happens for Gr sample survey (which was not doped). The presence of potassium on the graphene surface suggests that there might be a charge transfer due to the n-type doping, then graphene must have a negative superficial charge which becomes it into a more chemical reactive material likely to bond by electrostatic interaction.

The Table 5.1 shows the atomic percentages of the elements in each one of the four samples. From left to the right of the table the atomic percentage columns correspond to: Gr, K@Gr+O₂, K@Gr+H₂O and K@Gr+hex samples. In general, the four samples have carbon as the major constituent around 57 - 73% and oxygen and gold as minor constituents around 10 - 20% and 2 to 21.8% for each one. Given that the graphene layer is a pure material commercially obtained, then the presence of oxygen (as in survey spectra as atomic percentages) can only be attributed to the transferring process using PMMA due to all the samples have similar percentages and all the samples had this transferring process. This oxygen percentage around 10 - 20% suggests a slightly oxidation of graphene surface due to the PMMA interaction. Therefore, the oxygen attached to graphene surface must come from PMMA residues that were left after the removal process. The presence of gold is expected from the substrates which implies that the samples were thin enough verifying a superficial characterization.

Additionally, the survey and atomic percentages (Fig. 5.1 and Table 5.1) confirm the presences of other minor or trace elements as chlorine, iodine, sulfur and nitrogen; those elements have lower concentration about 3% on the sample surface and can be associated to contaminants. For instance, the nitrogen must be a common contaminant from the environment of synthesis given that all the samples have almost the same percentage, then it is a contaminant that all samples were exposed at the same time with same concentration. The contaminant could be caught at transferring process while the spin-coating, the drying at the fume hood, the acetone bath and the baking at the heating plates. The other trace elements as chlorine, iodide and sulfur might be attributed to the distilled water used during the synthesis process or functionalization process because those elements are part of the tap water used for the distillation. Then, those elements are residues at the distilled water. It means that the distilled water applied on graphene surface was not cleaned completely and had some trace elements. It can be verified with K@Gr+H₂O

Survey XPS - Atomic percentage of elements				
Sample	Gr	K@Gr+O ₂	K@Gr+H ₂ O	K@Gr+Hex
Element	Atomic Percentage (%)			
C1s	71.2	73.8	77.1	57.6
O1s	16.4	20.5	10.1	16.7
Au4f	8.5	2.4	6.0	21.8
N1s	3.1	2.3	2.2	3.1
K2p	<0.1	< 0.1	2.5	< 0.1
Cl2p	0.1	0.9	1.7	0.8
I3d5	-	<0.1	0.4	0.1
S2p	0.7	<0.1	< 0.1	< 0.1

Table 5.1: Atomic percentages of the elements found at the surface of the four different samples

sample where the water was used for the functionalization process and this sample has the highest concentrations of those contaminants. The water must have been triply distilled in order to avoid those contaminants on graphene surface.

In particular using the information from Figure 5.1 and Table 5.1:

- Gr sample shows a survey for a material pristine which only was transferred using PMMA. The presence of carbon is 71.2% corresponding to graphene monolayer. Also the presence of oxygen in a 16.4% of suggesting an barely oxidation attributed to the use of PMMA. Thus, a pure material (as a commercial) would show a survey with only one main and intensive peak and a high atomic percentage of the element. Therefore, the presence of oxygen must be subjected to the only interaction or modification made by the transferring process with the PMMA interaction. The polymer could have left residues whose oxygen atoms were attached to graphene surface, so all the samples have the similar concentrations of oxygen given that all were transferred using PMMA. In this way, the ratio of carbon to functional groups is 71.2:16.4 or equivalent to 4.34% of carbon per functional group which is the

degree of functionalization, taking into account one oxygen per functional group formed.

- K@Gr+O₂ sample survey spectrum shows the carbon contribution same as Gr sample but a higher peak contribution of oxygen than Gr sample or any other surveys, this is totally related to the type of exposure to which the sample was subjected (just O₂) and the oxidation from the synthesis method. The concentration of carbon and oxygen are around 73.8% and 20.5% respectively higher than in Gr sample.

At the survey does appear a potassium peak (K2p3 and K2s See Fig. 5.1 b) due to the doping process, this is an evidence that confirms a potassium deposition on graphene surface. Nevertheless, the atomic percentage of potassium is less than 0.1% for this sample (See Table 5.1). This could happen because the sample had an area of 1 cm² and the spot-size for the measurement was 100 μm, so the distribution of potassium was nonuniform through the surface, otherwise the potassium would not have been detected by the survey and high resolution spectra. Given that potassium was detected at the survey, C1s and O1s region but could not be quantified, it suggested a non uniform distribution of potassium ions by the annealing process. The potassium was guided by the gradient temperature without a homogeneous spread. In addition, even though the sample was exposed to O₂ is not a graphene oxide due to the concentration of oxygen is low. A graphene oxide would present a higher concentration of oxygen but this is not the case because the concentrations is a little higher than Gr sample, then the oxygen atoms are attached to specific places on graphene surface. In this way, the ratio of carbon to functional groups is 73.8:20.5 or equivalent to 3.6% of carbon per functional group which is the degree of functionalization, taking into account one oxygen per functional group formed.

- K@Gr+H₂O sample shows a material with a higher concentration of carbon 77.1% and lower concentration of oxygen 10.1%. Therefore, the sample was less oxidized in a environment with H₂O than in environment with O₂ but it is still oxidized likely due to the transferring process. The survey shows the photoelectron line (K2p3 and K2s See fig. 5.1 c) for potassium due to the doping process which confirms potassium deposition on graphene layer. For this sample, the potassium concentration is 2.5% in the analyzed sur-

face area. It means that the ratio of carbon to potassium is 77.1:2.5 or equivalent to 30.84% of carbon per potassium. Then, this is the doping degree of potassium. In the same way, the ratio of carbon to functional groups is 77.1:10.1 or equivalent to 7.63% of carbon per functional group which is the degree of functionalization, taking into account one oxygen per functional group formed.

- K@Gr+Hex sample shows a material with atomic percentage of 57.6% of carbon which is the lowest concentration of all the samples. This sample was also oxidized with the same percentage as Gr sample confirming that the oxidation is related to the transferring process. For this sample, it is important to highlight that the survey does not show potassium photoelectron line and the concentration is less than 0.1%. This means that even the sample was previously doped, the potassium was not detected at the survey or high resolution spectra due to the low concentration. Given that the other samples were successfully doped with potassium and measured, the deposition for this sample could be only affected by the type of exposure to which the sample was subjected. This is better explained in subsection 5.1.5. The peak contribution and atomic percentage of gold is bigger than in other surveys, this suggests that the measurement could be performed in a more uncovered area of material like on a shore. The ratio of carbon to functional groups is 57.6:16.7 or equivalent to 3.44% of carbon per functional group which is the degree of functionalization. However, the calculus of the degree of functionalization would not be appropriated for this region due to is a shore zone.

For a deeper analysis and a better understanding of surface interaction and bonds among graphene layer, PMMA, potassium element and the influence of the environment on the surface is required a high resolution analysis for C1s and O1s regions for each sample, to disclose the hidden interactions between the molecules and the graphene surface.

5.1.2 High resolution analysis of graphene pristine

First, the C1s region is analyzed and then the O1s region of Gr sample.

- **C1s region of Gr**

In Figure 5.2 a) shows the fitting of C1s region and presents five peaks. From the lower to higher binding energies, the first two peaks (red and purple color line) are centered at 284.69 and 285.20 eV corresponding to the carbon bonds with sp^2 hybridization characteristic for graphene and carbon bonds with sp^3 hybridization characteristic at edges and C-H bonds.²¹ The next three peaks (green, brown and pink lines) are centered at 286.27, 287.43 and 289.17 eV corresponding to single bonds C-O (epoxy and ether groups), double bonds C=O (carbonyl, quinones, ketones groups) and triple bonds O-C=O (carboxylic acids) respectively.^{21,27} Those results are summarized in Table 5.2

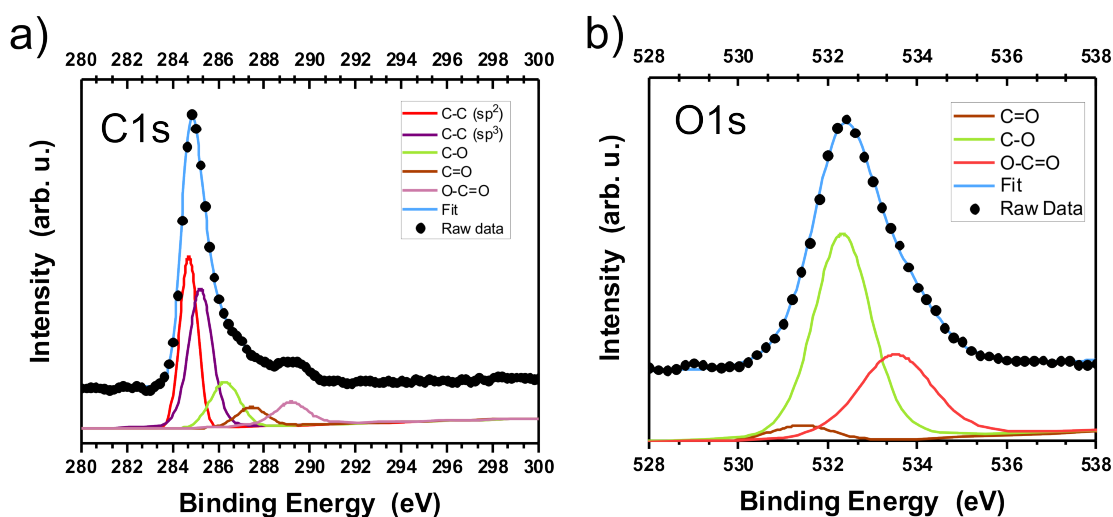


Figure 5.2: Fitting for measured spectra of graphene pristine sample. Deconvolution of C1s region (a) and O1s region (b).

If the sample would be pure graphene material, then the spectrum should present one narrow peak centered at 284.6 eV with a FWHM of 0.9 corresponding only to carbon sp^2 hybridization at C1s region, this would mean that the graphene does not have any functional groups or oxidation at the surface²⁸. However, this sample has five peaks related to carbon hybridization types and oxygen from the oxidation process as was explained in subsection 5.1.1. This sample has 71.2% of carbon and major contribution to the spectrum is from sp^2 and sp^3 hybridization carbon peaks. So, sp^2 carbon peak comes from the graphene layer structure and suggests a high quality material

because the peak is centered at the reported binding energy. The sp^3 carbon peak comes from the carbon atoms bonded at edges or possible defects on the surface caused by the oxidation process or the superficial interaction with PMMA. (See Table 5.2)

The intensity of carbon-carbon bond peaks are higher than the peaks related to oxygen groups, then these oxygen atoms originated from the transfer method are in less concentration (16.4%) and kept at surface without damaging the lattice structure. In addition, the peaks as C-O, C=O and O-C=O are associated to oxidation due to use of PMMA as transfer method. The chemical composition of the polymer has double bonds with oxygen and carboxylic acids. Hence, those peaks are functional groups attached to graphene surface originated from residues of PMMA after the removal process^{28,29}. Thereby, the single and double bonds corresponding to epoxy, carbonyl and carboxylic acid groups are most common structures attached in graphene³⁰. The removal process with acetone was not enough to eliminate all the residues related to the PMMA²⁹. In deed, to remove those oxygen atoms completely and clean the graphene surface it is needed an annealing process (until 500 °C) but this could break bonds and compromise the structure of graphene^{28,29}.

- **O1s region of Gr**

In Figure 5.2 b) shows the fitting of O1s region and has three peaks. The three peaks (brown, green and orange lines) are centered at 531.41, 532.32 and 533.50 eV corresponding to double bond C=O (carbonyl, quinones groups), single bond C-O (epoxy groups) and triple bond O-C=O (carboxylic acid groups) respectively.^{21,27} Those results are according to the single and double bonds between carbon and oxygen found at C1s region fitting (See Table 5.2).

Thus, those peaks confirm the presence of oxygen atoms bonded at the surface of graphene becoming into an barely oxidized graphene. The C=O peak is related to carbonyl groups at the edges of the graphene structure which are part of possible defects formed. The C-O peak has the major intensity and contribution on the fitting. Therefore, most of the 16.4% of oxygen are single bonded with carbon as in epoxy or ether groups. Oxygen atoms are most favorable to be adsorbed at bridge position over carbon-carbon bonds than C=O or O-C=O groups. So, oxygen

Region	Assignment	BE (eV)	RBE (eV)	Assignment
C1s	C-C sp ²	284.69	284.5 ²¹	C-C (sp ²) ²¹
C1s	C-C sp ³	285.20	285.2 ²¹	C-C sp ³ ; C-H ²¹
C1s	C-O	286.27	286.3 ²⁷	ether, epoxy groups ²⁷
C1s	C=O	287.43	287.4 ²¹	carbonyl, quinones groups ²¹
C1s	O-C=O	289.17	289.1 ²¹	carboxylic acid groups ²¹

Region	Assignment	BE (eV)	RBE (eV)	Assignment
O1s	C=O	531.41	531.1 ²¹	carbonyl, quinone groups ²¹
O1s	C-O	532.32	532.15 ²⁷	epoxy groups ²⁷
O1s	O-C=O	533.50	533.38 ²⁷	carboxylic groups ²⁷

*BE.- binding energy used for the fitting. RBE.- reported binding energy.

Table 5.2: Assignment of peaks for C1s and O1s regions for graphene pristine sample.

atoms are integrated at the graphene network becoming graphene layer sample into an oxidized graphene.^{30,31} The O-C=O peak is related to carboxylic acids which also comes from possible defects of the graphene structure. The three peaks of the fitting at the O1s region agree with each type of bonds presented in C1s region fitting verifying the presence of those functional groups originated from PMMA residues, oxidation and possible defects.

In summary, this sample has oxygen due to functional groups by the residues of PMMA after the transferring method. The presence of functional groups can alter the van der Waals interactions of graphene, graphene could change its interaction with the environment as increasing the solubility, specially due to the presence of C=O and O-C=O groups which give a slightly hydrophilic character¹⁰.

5.1.3 High resolution analysis of potassium-doped graphene exposed to O₂

This graphene sample was transferred to an Au wafer by using PMMA, doped with potassium by an annealing process and exposed to air in a glove box as it was explained in Chapter 4.1. First, the C1s region is analyzed and then the O1s region of K@Gr+O₂ sample.

- **C1s region of K@Gr+O₂**

In Figure 5.3 a) shows the fitting of C1s region and presents six peaks. From the lower to higher energies, the first two peaks (red and purple lines) are centered at 284.68 and 285.45 eV corresponding to carbon bonds with sp² hybridization characteristic for graphene and carbon bonds with sp³ hybridization characteristic at edges and C-H bonds²¹. The next two peaks (brown and pink lines) are centered at 287.43 and 289.04 eV corresponding to double bonds C=O (carbonyl, quinones groups) and triple bonds O-C=O (carboxylic acids groups).²¹ The last two peaks (fuchsia and cyan lines) are centered at 292.71 eV (K 2p_{3/2}) and 295.40 eV (K 2p_{1/2}) corresponding to K oxides (potassium oxides) and K⁺ cations (potassium cations) due to spin-orbit split doublet.³² Those results are summarized in Table 5.3

Same as the Gr sample, the C1s region of this sample shows four peaks related to carbon hybridization types and the oxygen in the functional groups from PMMA residues, this sample indicates a higher oxidation (20% of oxygen) originated from the transferring process and the

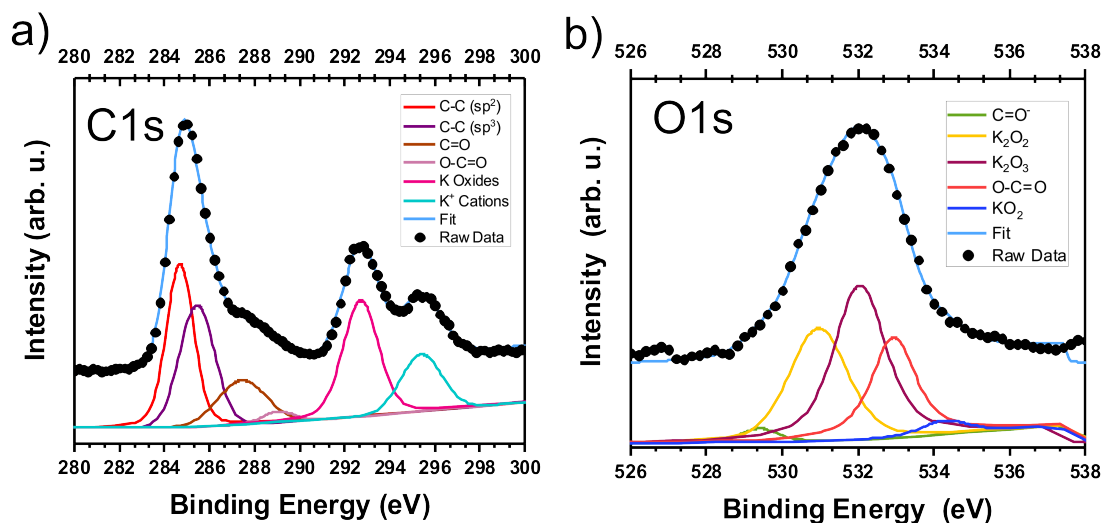


Figure 5.3: Fitting for measured spectra of potassium-doped graphene samples exposed to air. Deconvolution of C1s region (a) and O1s region (b).

environment. From the 73.8% of carbon, the major contribution to the spectrum is from sp^2 and sp^3 hybridization carbon peak. The intensity of sp^2 carbon peak suggests a high quality material. However, the sp^3 carbon peak comes from carbon atoms bonded at edges or possible defects on the surface caused by the PMMA.

The intensity of the carbon-carbon peaks are higher than the intensity of the functional groups peaks, then the surface is oxidized (20%) but it does not damage the lattice structure. As in Gr sample, the C=O and O-C=O peaks are associated to the oxidation caused by the PMMA residues from the transfer method and also due to oxygen from the environment where the sample was exposed. Additionally, C1s region shows two potassium peaks which are the proof of the deposition of the metal ions by doping process as the survey spectrum suggested (See Fig. 5.1). This is a noncovalent functionalization because the graphene structure was not affected by the doping and air exposure processes based on the peak for carbon bonds with sp^2 and sp^3 hybridization which are high in intensity and are centered in similar range of binding energies as the reported values (See Table 5.3). The noncovalent functionalization is produced by a cation- π interaction due to an electrostatic interaction and induction of energies caused by the positively charged cations and the

negatively charged π electron cloud from graphene. So, the potassium cations donate their outer s-electrons to graphene system and they are integrated at surface through ionic bond (Coulombic interactions) at the hollow site over the honeycomb carbon arrangement.^{23,24}

At this point, it is important to mention that the potassium peaks are two types: cations and oxides. The cations contribute with the charge transfer interactions between potassium atoms and graphene. The oxides are formed because of potassium is a highly reactive alkaline metal and can cause the migration of oxygen atoms through the surface to form an oxidized interfacial layer or take oxygen from environment.²² The oxygen migration must be related to the high reactivity of potassium (high redox potential) that can attract oxygen single bonded. In comparison with C1s region of Gr sample, the C-O peak disappeared and could be attributed to the fact that the oxygen atoms at the surface migrated through the surface to react with potassium by forming potassium oxides unlike than the oxygen atoms from C=O and O-C=O groups which are more stable bonded with carbon (the real contribution of possible defects of this sample surface).

- **O1s region of K@Gr+O₂**

In Figure 5.3 b) shows the fitting of O1s region and presents five peaks. From lower to higher binding energies, the first peak (green line) is centered at 529.4 eV corresponding to a semiquinone C=O⁻ or a more complex oxidizing group.³¹ The next two peaks (yellow and lilac lines) are centered in 530.95 and 532.05 eV corresponding to potassium peroxide K₂O₂ and potassium sesquioxide K₂O₃.³³ The two last peaks (orange and blue lines) are centered at 532.93 and 534.4 eV corresponding to non-carbonyl oxygen atoms O-C=O and potassium superoxide KO₂.^{21,33} Those results are according to the double bonds between carbon and oxygen and the K 2p peaks found at C1s region fitting. (See Table 5.3).

Since the sample has PMMA residues and was exposed to air, the concentration of oxygen is higher than Gr sample about 20%. It means that the O1s region has more oxide species because of the excess of oxygen atoms (O₂) that reacted at the surface sample. The first peak of O1s region is centered at 529.4 eV, this peak is not reported in literature for graphene oxide samples but the peak could be attributed to oxygen bonded to unsaturated carbon atoms at edges (armchair

Region	Assignment	BE (eV)	RBE (eV)	Assignment
C1s	C-C sp ²	284.68	284.5 ²¹	C-C (sp ²) ²¹
C1s	C-C sp ³	285.45	285.2 ²¹	C-C (sp ³); C-H ²¹
C1s	C=O	287.43	287.4 ²¹	carbonyl, quinones groups ²¹
C1s	O-C=O	289.04	289.1 ²¹	carboxylic acids groups ²¹
C1s	K oxides	292.71	292.8 ³²	K oxides (K 2p _{3/2}) ³²
C1s	K ⁺ cations	295.40	295.8 ³²	K cations (K 2p _{1/2}) ³²
Region	Assignment	BE (eV)	RBE (eV)	Assignment
O1s	C=O ⁻	529.40		semiquinona ³¹
O1s	K ₂ O ₂	530.95	531.0 ³³	potassium peroxide ³³
O1s	K ₂ O ₃	532.05	532.0 ³³	potassium sesquioxide ³³
O1s	<u>O</u> -C=O	532.93	533.1 ²¹	non-carbonyl groups ²¹
O1s	KO ₂	534.3	534.3 ³³	superoxide ³³

*BE.- binding energy used for the fitting. RBE.- reported binding energy.

Table 5.3: Assignment of peaks for C1s and O1s regions for potassium-doped graphene sample exposed to air.

or zigzag) or vacancies sites where semiquinone or carbonyl groups are formed.³¹ Then, the peak at 529.4 eV could be attributed to oxidizing groups as semiquinone (free radical, oxidant and unstable) because C=O groups (or more complex structures) are predicted to appear toward lower binding energies than carbonyls (531.1 eV²¹).³⁰ Therefore, according to the C1s region fitting, the functional groups that appeared at the edges in possible defects are the carbonyl or carboxylic acid groups. So, it is more likely the peak corresponds to semiquinones to appear at the graphene sample surface due to the range of energy of the peak.

The O-C=O peak is related to the carboxylic acids. The semiquinone and carboxylic acid peaks have same origin from PMMA residues due to the transfer method. The formation of these functional groups contribute to the possible defects of graphene structure and confirm the graphene oxidation.

In addition, the O1s region presents different types of oxidized potassium as: potassium oxide (K₂O₂), potassium sesquioxide (K₂O₃) and potassium superoxide (KO₂) due to the excess of oxygen and are centered to the reported energies (See Table 5.3). Since, the potassium is highly reactive because is a strong reducing agent, the potassium reacted with the all types of oxygen atoms from the environment and surface. In this way, potassium could react with oxygen single bonded to carbon and caused a migration oxygen atoms at surface as was suggested in C1s region.²² Likewise, potassium has control over the reactive oxygen intermediates production by the formation of discrete complexes. Thus, potassium can support the series of oxygen reduction toward other more reactive species via one electron transfer reactions as catalysts in the oxygen activation.³⁴ In this way, many of the potassium ions could be oxidized with different reduced oxygen species by forming different type of oxides. From them, the K₂O₃ peak contributes more to the fitting because of the exposure of K-doped graphene to a high content of oxygen. On the other hand, K⁺ cations can exist by the negatively charged groups as semiquinones or negatively charged π orbits which stabilize the charges at the graphene surface.

In summary, this sample has a highest oxidation and degree of functionalization with functional groups. The atomic percentage might not be measured due to a non uniform deposition of potassium on graphene surface. Nevertheless, the high resolution spectra in C1s and O1s region confirm the presence of potassium dispersed on graphene surface without affecting the

network as it is suggested on literature^{14,35}. Then, the metal acts as charge transfer dopant, also interacting with oxygen atoms from the environment because potassium can support the oxygen reductions. Therefore, potassium allows a higher functionalization with oxygen and formation of oxide species. In this way, the graphene is n-type doped which changes it into a negatively charged surface but the sample is not a conductive one because the spectrum has symmetric peaks. Then the functional groups must be responsible for avoiding the electron conduction from potassium to graphene and through graphene surface. So the material keeps as semiconductor by the functional groups that can induce holes or make a p-type material depending on the amount of functional groups at the surface. Also, the higher functional groups can affect the van der Waals interactions changing graphene reactivity, increasing the solubility due to the presence of C=O and O-C=O which increase the hydrophilic character¹⁰.

5.1.4 High resolution analysis of potassium-doped graphene exposed to H₂O

This graphene sample was transferred to an Au wafer by using PMMA, doped with potassium by an annealing process and exposed to distilled water in a glove box as it was explained in Chapter 4.1. First, the C1s region is analyzed and then the O1s region of K@Gr+H₂O sample.

- **C1s region of K@Gr+H₂O**

In Figure 5.4 a) shows the fitting of C1s region and presents five peaks. From the lower to higher binding energies, the first two peaks (red and purple lines) are centered at 284.67 and 285.14 eV corresponding to carbon bonds with sp² hybridization characteristic for graphene and carbon bonds with sp³ hybridization characteristic at edges and C-H bonds.²¹ The next peak (pink line) is centered at 288.31 eV corresponding to an overlapping of ketones and carboxyls.³⁶ The last two peaks (fuchsia and cyan lines) are centered at 292.9 eV (K 2p_{3/2}) and 295.70 eV (K 2p_{1/2}) corresponding to K oxides (potassium oxides) and K⁺ cations (potassium cations) due to the spin-orbit split doublet.¹⁴ Those results are summarized in Table 5.4.

Same as the Gr and K@Gr+H₂O samples, the C1s region shows three peak related to carbon hybridization types and functional groups coming from the PMMA residues. This sample has

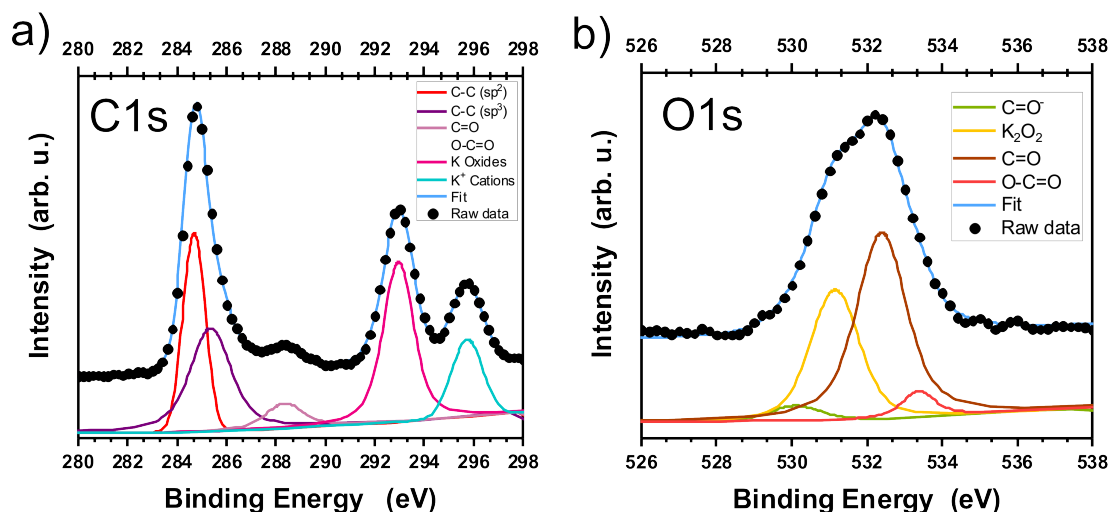


Figure 5.4: Fitting for measured spectra of potassium-doped graphene samples exposed to water. Deconvolution of C1s region (a) and O1s region (b).

77.1% of carbon and the major contribution to the spectrum is from sp^2 and sp^3 hybridization carbon peaks. The sp^2 carbon peak comes from the graphene layer structure and suggests a high quality material because the peak is centered to the reported value. This means that the doping process and the exposure to water does not affect the graphene layer structure. The sp^3 carbon peak comes from carbon atoms bonded at the edges or possible defects on the surface. (See Table 5.4)

This sample was exposed to H_2O but the oxidation was less than the samples (10.1%). So, those oxygen atoms in functional groups in C1s region were originated from PMMA residues during the transferring method as in previous samples. It is important to mention that the third peak at 288,31 eV cannot be attributed to either ketones nor carboxyl groups because the peak is located at a binding energy right at the middle of reported binding energies for both groups. It means that the peak is the result of the contribution from the two functional groups, as a sum of an overlapping between C=O (carbonyl, ketones groups) and O-C=O (carboxylic acid groups).³⁶ This is unusual peak can be better defined with a higher energy resolution step and acquisition time in order to distinguish between the two peaks.

Also, the C1s region shows the peaks related to the potassium doping. Those peaks demonstrate the noncovalent functionalization between potassium ions and graphene layer without affecting the structure. The potassium cations were functionalized at graphene surface by the cation- π interaction due to the coulombic interaction same as in K@Gr+O₂ sample.²⁴ In the same way, potassium cations contribute to the charge transfer interactions by donating the outer s-electrons to π system and some potassium ions reacted and formed oxides with oxygen from the environment or the migrated oxygen atoms single bonded with carbon at the surface.²² In addition, the concentration of oxygen was less than for air samples, then the potassium ions can react with the most favorable reduced oxygen species and the rest of ions will keep as cations on the graphene surface. This is the reason why the potassium peaks are more intense when compared to samples.

- **O1s region of K@Gr+H₂O**

In Figure 5.4 b) shows the fitting of O1s region and presents four peaks. From lower to higher energies, the first peak (green line) is centered at 530.1 eV corresponding to a semiquinone C=O⁻ or a more complex oxidizing groups.³¹ The next peak (yellow line) is centered at 531.15 eV corresponding to potassium peroxide K₂O₂.³³ The last two peaks (brown and orange lines) are centered at 532.39 and 533.37 eV corresponding to double bond C=O (carbonyl, quinones groups) and triple bond O-C=O (carboxylic acid groups) respectively. Those results are according to the bonds between carbon and oxygen and the K 2p peaks found at C1s region fitting (See Table 5.4).

Given the peak assignment for this region, the four peaks are related to the PMMA residues and the environment where the sample was exposed. This sample has less oxidation due to less source of oxygen. The first peak at 530.1 eV is not reported in literature but it could be attributed to oxygen bonded to unsaturated carbon atoms at edges or vacancies sites where semiquinones or more complex oxidizing group can be formed.³¹ This peak is attributed to a semiquinone because C=O groups are predicted to appear toward lower binding energies than carbonyls as in the case of K@Gr+O₂.³⁰ In addition, the presence of groups as C=O⁻, C=O and O-C=O peaks confirm the presence of oxygen atoms bonded at the sample surface at edges or as part possible defects coming from PMMA residues due to the transfer method. Those peaks are in agreement to the

Region	Assignment	BE (eV)	RBE (eV)	Assignment
C1s	C-C sp ²	284.67	284.5 ²¹	C-C (sp ²) ²¹
C1s	C-C sp ³	285.14	285.2 ²¹	C-C sp ³ ; C-H ²¹
C1s	C=O and O-C=O	288.31	288.2 ³⁶	overlap ketones and carboxyls ³⁶
C1s	K oxides	292.95	292.8 ³²	K oxides (K 2p _{3/2}) ³²
C1s	K ⁺ cations	295.70	295.8 ³²	K cations (K 2p _{1/2}) ³²

Region	Assignment	BE (eV)	RBE (eV)	Assignment
O1s	C=O ⁻	530.10		semiquinona ³¹
O1s	K ₂ O ₂	531.15	531.0 ³³	potassium peroxide ³³
O1s	C=O	532.39	532.2 ²¹	carbonyl, quinone groups ²¹
O1s	O-C=O	533.37	533.38 ²⁷	carboxylic acid groups ²⁷

*BE.- binding energy used for the fitting. RBE.- reported binding energy.

Table 5.4: Assignment of peaks for C1s and O1s regions for potassium-doped graphene sample exposed to water.

C1s region fitting.

Unlike than the previous O1s region for K@Gr+O₂, this sample has less types of reduced oxygen atoms because most of them are bonded to hydrogen and the available ones are single bonded with carbon or in molecular form. In this way, the oxygen atoms must reach an excited state by electron transfer reaction (oxygen activation) using the same potassium ions to reduce oxygen into species thermodynamically favorable to form potassium oxides.³⁴ Those facts lead to assume that the most reactive or less stable specie is O₂²⁻ and will react with the potassium ions. This could be the reason to the presence of only potassium peroxide K₂O₂ peak. This is the only potassium oxide specie formed on contrary to O1s region for K@Gr+O₂ which has more oxide types.

In addition, the potassium ions peak is more intensive due to their stabilization by the graphene structure and semiquinone group. There was an increase in intensity of the semiquinone and K⁺ cation peaks, both can be proportionally related due to the charge of K cations could be stabilized with the semiquinones and the π orbitals.

In summary, this sample has a lower oxidation and functionalization with oxygen due to the environment was more stable than in K@Gr+O₂. The C1s and O1s region spectra confirm the deposition of potassium on graphene sample without affecting the network. Then, the potassium acts as charge transfer dopant interacting with the likely reduced oxygen atoms to form potassium oxides. In this way, potassium allows a functionalization only when likely oxide species are formed. Also, the graphene is n-type doped which changes it into a negatively charged surface but this is not a conductive material because the spectrum has symmetric peaks, then the functional groups affect the electron conductivity. Besides, the functional groups as C=O and O-C=O can alter the van der Waals interactions of graphene changing it into a more soluble with slightly hydrophilic character¹⁰.

5.1.5 High resolution analysis of potassium-doped graphene exposed to hexyliodide

This graphene sample was transferred to an Au wafer by using PMMA, was doped with potassium by an annealing process and exposed to a drop of hexyliodide in a glove box as it was explained in Chapter 4.1. First, the C1s region is analyzed and then the O1s region of K@Gr+Hex sample.

- **C1s region of K@Gr+Hex**

In Figure 5.5 a) is shown the fitting of C1s region and presents five peaks. From the lower to higher binding energies, the first two peaks (red and purple lines) are centered at 284.5 and 285.2 eV corresponding to carbon bonds with sp^2 hybridization characteristic for graphene and carbon bonds sp^3 hybridization characteristic at edges and C-H bonds.²¹ The next three peaks (green, brown and pink lines) are centered at 285.91, 287.02 and 288.66 eV corresponding to single bonds C-O (hydroxyl, phenolic groups), double bonds C=O (carbonyl, quinones, ketones groups) and triple bonds O-C=O (carboxylic acids) respectively.^{22,37} Those results are summarized in Table 5.5

Same as in Gr, K@Gr+O₂ and K@Gr+H₂O, the C1s region shows peaks related to carbon hybridization types and functional groups caused due to PMMA residue. This sample has 57.6% of carbon (the lowest concentration of all samples) and 21.8% of gold (highest concentration of all samples) suggesting that the measurement was performed in a uncovered area as a shore. The atomic percentages are different than the other samples with similar synthesis process. From the 57.6% of carbon, the major contribution to the spectrum of C1s is from sp^2 carbon peak. The intensity of the peak suggests a higher quality of the material than for the case of other samples (even the Gr sample). Moreover, the intensity of sp^3 carbon peak decreased compared to the other samples, so the carbon atoms bonded at edges or possible defects decreased on the surface. Given that this sample was also transferred using PMMA (which causes oxidation and possible defects in the previous samples), then the change in peak intensities can be related to the hexyliodide exposure. Therefore, hexyliodide molecule could recover and improve the graphene structure (higher intensity of sp^2 carbon peak) and reduce the defects compared to the three previous samples (lower intensity of sp^3 carbon peak).

The intensity of the peak related to oxygen is lower than the carbon-carbon bond peak intensity. The sample is oxidized (16.7%) and the oxygen atoms are related to the presence of functional groups attached at the surface. In this way, the peaks of functional groups corresponding to C=O and O-C=O originated from PMMA residues but the C-O peak is related to phenol or hydroxyl groups (C-OH) originated from the hexyliodide compound and is not related to epoxy groups^{37,38}. In this way, the aliphatic chain from hexyliodide was attached to graphene surface without damaging it. In addition, all those functional groups peaks are centered at lower binding energies compared to graphene pristine sample which could be attributed to vacancies or distortions at lattice³⁰.

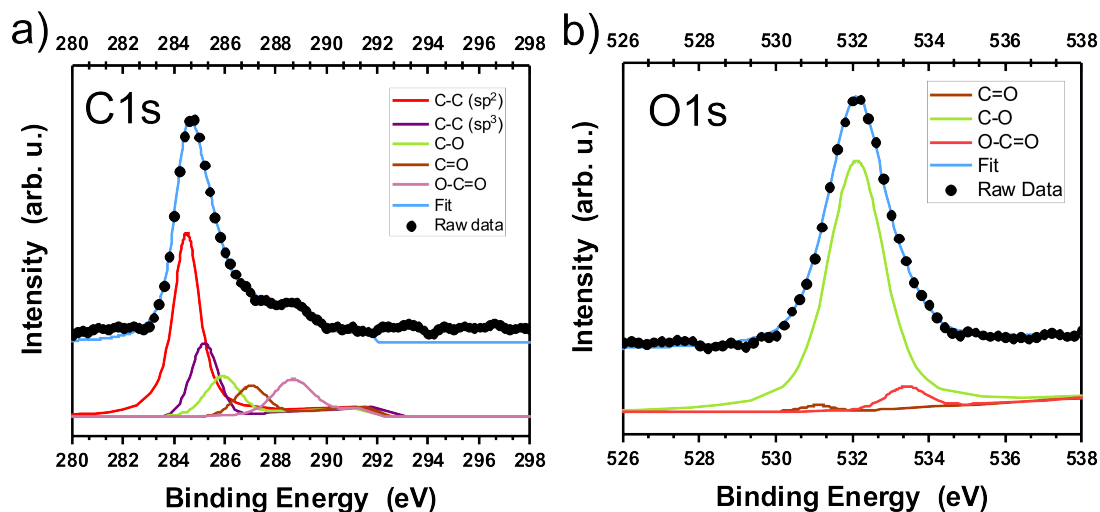


Figure 5.5: Fitting for measured spectra of potassium-oped graphene samples exposed to hexyliodide. Deconvolution of C1s region (a) and O1s region (b).

Even though this sample was doped with potassium, the potassium peak do not appear in the C1s region or in the survey spectrum (See Fig. 5.1). The absence of potassium peaks means that this graphene sample is not functionalized anymore with potassium ions. So, if the potassium ions were functionalized at the graphene lattice by electrostatic interactions, then they only could be removed due to a stronger coulombic interaction. Since the two previous samples were functionalized with the doping process, then the hexyliodide must be responsible for the

absence of potassium ions. It could happen that the iodide atoms from the hexyliodide compound must react with potassium ions forming ionic bonds as a result of ion-ion interaction. In this way, all the iodide atoms reacted with all potassium ions due to its high electronegativity forming potassium iodide salt. Due to the resulting salt does not appear at the survey or C1s spectrum, it is not functionalized with the graphene structure at all. The atomic percentages of potassium and iodide are around 0.1%, then the resulting salt should be placed not homogeneously on the surface and can not be measured properly. Moreover, the iodide salts are ascribed to lead a selective abstraction of the epoxies oxygen (C-O-C) present in the graphene oxide causing a reduction of the defects but also causes an increment in the formation of phenol groups (C-OH)³⁶. Therefore, the hexyliodide caused: the formation of potassium iodide (by removing the potassium from graphene surface) and an improvement in graphene structure by recovering from the doping process. The potassium iodide helped to remove the epoxy oxygen atoms as a consequence the functional groups were centered to lower binding energies due to vacancies and the C-O peak is attributed to C-OH groups³⁶.

- **O1s region of K@Gr+Hex**

In Figure 5.5 b) shows the fitting of O1s region and presents three peaks. The three peaks (brown, green and orange lines) are centered at 531.09, 532.10 and 533.4 eV corresponding to double bond C=O (carbonyl, quinones groups), single bond C-O (aliphatic carbon) and triple bond O-C=O (carboxylic acid groups) respectively^{27,38}. Those results are according to the single and double bonds between carbon and oxygen found at C1s region fitting (See Table 5.5)

The O1s region does not present a peak related to potassium oxide. The absence of potassium oxide peaks or iodine oxides interaction confirms that potassium ions are not functionalized with the graphene structure and interacted with the iodine. Since the sample had PMMA residues, the oxygen atoms are part of functional groups as carbonyl and carboxylic acid groups (C=O and O-C=O) which are part of defects but those peak are less intense than for Gr sample, then this sample has a less defective structure. For this sample, the C-O peak is attributed to oxygen bonded to aliphatic carbon structure due to the presence of the hexyliodide chain.³⁸ Thus, the peak has the major intensity and contribution on the fitting because the hexyliodide was spread over all the graphene surface. Besides, the C-O are more likely attributed to hydroxyls or phenols because the presence of iodide potassium contributes to a reorganization of the system by

Region	Assignment	BE (eV)	RBE (eV)	Assignment
C1s	C-C sp ²	284.5	284.5 ²¹	C-C (sp ²) ²¹
C1s	C-C sp ³	285.2	285.2 ²¹	C-C sp ³ ; C-H ²¹
C1s	C-O	285.91	286.0 ³⁸	hydroxyl, phenolic groups ^{38,37}
C1s	C=O	287.02	287.0 ²²	carbonyl, quinone groups ²²
C1s	O-C=O	288.66	288.8 ³⁷	carboxylic acid groups ³⁷
Region	Assignment	BE (eV)	RBE (eV)	Assignment
O1s	C=O	531.09	531.08 ³⁸	carbonyl, quinone groups ³⁸
O1s	C-O	532.10	532.03 ³⁸	aliphatic carbon-oxygen ³⁸
O1s	O-C=O	533.4	533.3 ²⁷	carboxylic acid groups ²⁷

*BE.- binding energy used for the fitting. RBE.- reported binding energy.

Table 5.5: Assignment of peaks for C1s and O1s regions for potassium-doped graphene sample exposed to hexyliodide.

removing the oxygen atoms (deoxygenate) and causing the formation of phenol groups³⁶. In this way, the amount of oxygen atoms for this samples was reduced and few of them remained at edges.

In summary, this sample shows a recovery of its structure after the doping process. Then, this sample confirms that the potassium was noncovalent functionalized with graphene (as in the other samples) because the iodide took away the potassium ions by stronger electrostatic interactions once they interacted each other. So, the potassium was attached to graphene surface by electrostatic interaction but when it was removed, did not destroy or alter the graphene network. Also, the hexyliodide molecule helps with a deoxygenation of the sample reducing the possible defects, improving its structure.

Finally, The four samples presented different results. Gr sample had a slight oxidation due to PMMA residues attached on graphene surface with a degree of functionalization of 4.34% of carbon per functional group. K@Gr+O₂ showed potassium deposition in a non uniform distribution. The environments and potassium ions increased the oxidation and functionalization transforming graphene into a more reactive material with a 3.6% of carbon per functional group. K@Gr+H₂O showed potassium deposition but the environment was less oxidizing, then potassium contributed with the formation of specific oxide species. The formed functional groups can make graphene a reactive material but less than in the previous sample with 7.63% of carbon per functional group. Both previous samples showed that potassium was attached to graphene surface without affecting it (noncovalent functionalization) driving by electrostatic forces. The K@Gr+Hex synthesis showed a recovery of graphene without the presence of potassium and less functional groups due to the hexyliodide molecule which improves the graphene characteristics of the material. This could mean a method for recovering and improving the graphene material after a doping with alkali metals and reducing the defects.

At the end, these samples were n-type doped but the peaks were symmetric at the fitting spectra showing a non conductive materials due to the functional groups that might influence on charge transport. The graphene kept as semiconductor without conductive behavior. If the synthesis is improved in order to avoid the functional groups and PMMA residues, then the graphene could have potential future applications in electronic devices as batteries. At the same

time, the amount of carboxylic, carbonyl groups and other functional groups can alter the van der Waals interactions and increase the solubility of graphene in organic solvents. This might lead to potential future applications for graphene with more biocompatible properties useful for biological systems¹⁰.

5.2 MWCNTs sample

5.2.1 Elemental analysis of MWCNTs sample

In Figure 5.6 is presented the survey for MWCNTs sample. The survey presents two photoelectron lines, the main and most intensive one corresponding to carbon element and secondary one corresponding to oxygen. There is not presence of any other element at the sample surface neither the catalysts nor the substrate. In Table 5.6 shows the atomic percentage of the elements in the sample. The major constituent is carbon with 98% which means that the material is highly pure and the synthesis method for the nanotubes is effective for a growth of carbon nanotubes without contaminants as catalysts or substrate residues encapsulated.¹⁵ This suggests that the CaCO_3 is an excellent support as substrate for MWCNTs production by catalysis because of the synthesized nanotubes do not required any extra process for removal of contaminants or purification. The MWCNTs are very stable and low reactive with other elements. In addition, the oxygen has a concentration of 1.2%, it could be related related to the chemical decomposition of CaCO_3 .¹⁵

For a better understanding of the surface interactions it is required an analysis of C1s and O1s region.

5.2.2 High resolution analysis of MWCNTs

- C1s and O1s regions of MWCNTs analysis

In Figure 5.7 a), it is presented the fitting for spectrum of C1s region. The fitting has three peaks centered at 284.76, 286.05 and 290.6 eV corresponding to carbon bond with sp^2 hy-

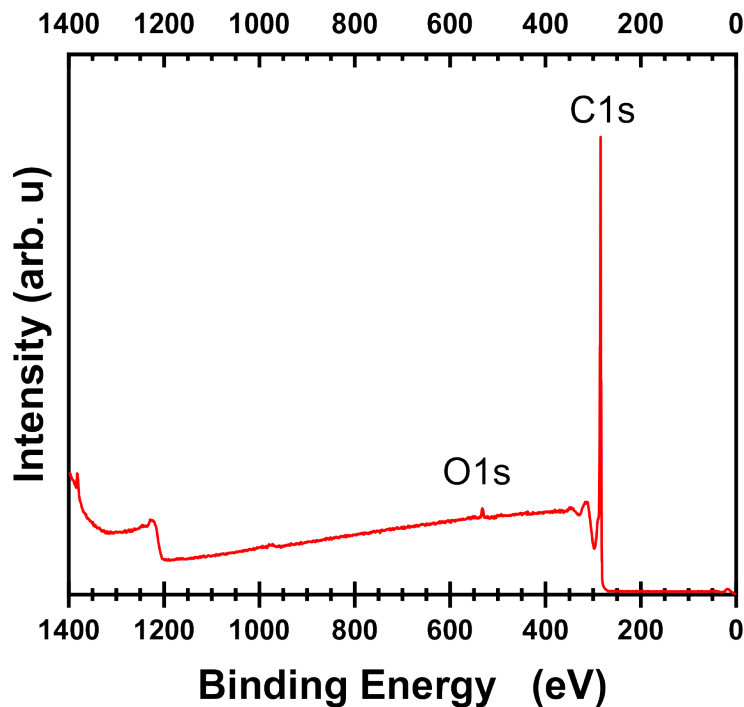


Figure 5.6: Survey spectrum for MWCNTs pristine

bridization, single bond C-O and $\pi - \pi^*$ transition.^{27,39} Those peaks are summarized in Table 5.7. The first peak has the major contribution for C1s region spectrum which implies that most of 98% carbon elements have this type of hybridization in MWCNTs. However, the peak is shifted to 284.7 eV in comparison to 284.5 eV from graphene in a flat structure.^{15,21} The shift is caused by the tubular structure of nanotubes which leads to a distortion of the bond and a shift in binding energy despite of the carbon atoms have sp^2 hybridization. Additionally, this peak had an asymmetric characteristic. Therefore, the fitting was performed using a DonaichSunjic function instead of a Voigt function. For the previous fittings were used Voigt functions because the peaks were symmetric. Nevertheless, DonaichSunjic functions are always used for asymmetric peaks, this characteristic commonly corresponds for metal materials. Therefore, the asymmetry characteristic of this peak demonstrates a metallic behavior of the MWCNTs as would be expected. In consequence, the informa-

Survey XPS - Atomic percentage of elements	
Sample	MWCNTs
Element	Atomic Percentage (%)
C1	98.6
O1s	1.2
Co2p3	0.1
Ca2p	0.1
Ar2p	< 0.1
Fe2p3	< 0.1

Table 5.6: Atomic percentages of the elements present at MWCNTs pristine samples

tion of this peak suggests that the MWCNTs are highly pure with sp^2 hybridization, with high quality and metallic behavior based on the peak contribution and the nature of the peak.

The second and third peak were fitted with Voigt functions. The second peak is related to single bonds C-O due to the presence of oxygen atoms possibly coming from the substrate. Some studies agreed that the $CaCO_3$ can decompose at $700\text{ }^\circ\text{C}$ to CaO and produce CO_2 .¹⁵ So, the C-O comes from CO_2 or CaO which could be attached at MWCNTs surface. The survey and atomic percentage of oxygen shows a low the concentration of oxygen, so the C-O peak has low intensity.

It is important to mention that the high purity of the MWCNTs could be attributed to due production of CO_2 , some studies agreed that CO_2 can act as an etching agent to avoid the encapsulation of catalyst particles.¹⁵ Therefore, it improves the yield of reaction and quality of the MWCNTs produced. The third peak is related to $\pi - \pi^*$ transition corresponding to shake-up line. The peak intensity is related to the sp^2 carbon content, also it can be associated to the metallic behavior of the sample.

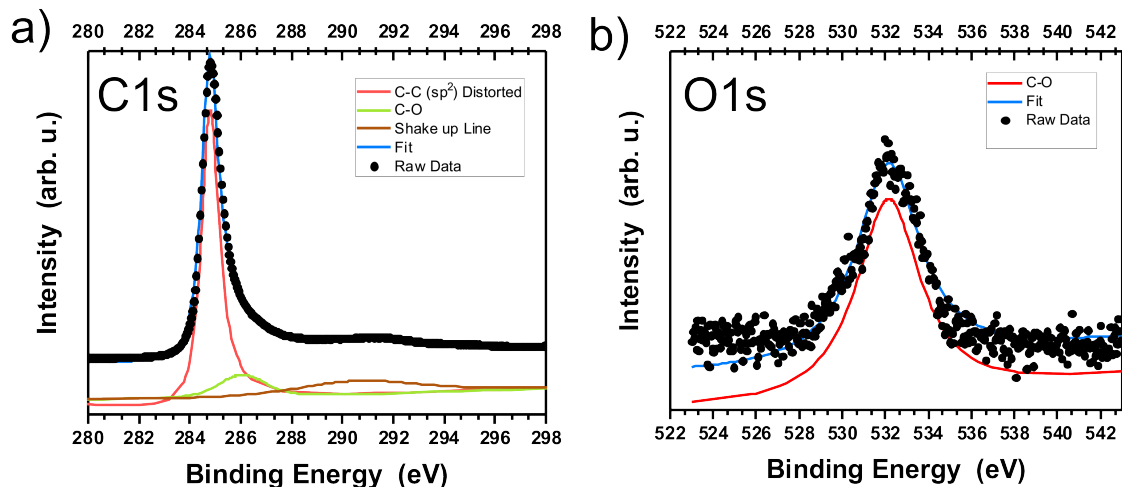


Figure 5.7: Spectra measured for MWCNTs pristine. Deconvolution of C1s region (a) and O1s region (b)

In Figure 5.7 b), it is presented the fitting for spectrum of O1s region. The fitting has one peak centered at 532.15 eV (See Table 5.7). This peak corresponds to C-O bond which is attribute to the decomposition of $CaCO_3$ substrate as was explained previously.^{15,39} This is the only peak given that there is not other type of interactions between MWCNTs structure and oxygen. For the fitting the major contribution was from the Lorentzian width at the Voigt function.

Finally, MWCNTs show a survey without contaminants and with a high intense peak related only to carbon. This is a survey for conductive and pure material unlike than the survey for graphene samples which have the presence of other elements from contaminant and also the contribution for the background due to loss of energy from emitted photoelectrons of lower kinetic energy due to they were not a conductor as good as MWCNTs are. Besides, the high resolution spectra for MWCNTs have peaks centered to reported data with a sharp form which means the absence of any other functional group attached to MWCNTs surface as it happens for graphene samples. Then, MWCNTs are pure material which can be used as a reference to compared with functionalized materials to differentiate the spectrum from a pure materials to a functionalized one.

Region	Assignment	BE (eV)	RBE (eV)	Assignment
C1s	C-C sp ²	284.76	284.7 ³⁹	C-C (sp ²) ³⁹
C1s	C-O	286.05	286.3 ²⁷	ether, epoxy groups ²⁷
C1s	$\pi - \pi^*$	290.6	290.6 ²¹	Shake up lines ²¹
Region	Assignment	BE (eV)	RBE (eV)	Assignment
O1s	C-O	532.15	532 ³⁹	epoxy groups ³⁹

*BE.- binding energy used for the fitting. RBE.- reported binding energy.

Table 5.7: Assignment of peaks for C1s and O1s regions for MWCNTs sample

Chapter 6

Conclusions & Outlook

This investigation analyzed graphene functionalized with potassium and MWCNTs using XPS as characterization technique to understand the interactions at the surface of each sample. The results were presented by an elemental and surface analysis to understand the chemical composition and the bond type on the surface samples. The results were obtained for graphene samples and MWCNTs sample.

- **Functionalized graphene sample**

There were four graphene samples: Gr, K@Gr+O₂, K@Gr+H₂O and K@Gr+Hex. All they presented carbon as major constituent and oxygen as minor constituent. Due to the presence of oxygen, it is assumed that the graphene monolayers commercially obtained were oxidized around 10 - 20% due to the transferring process with PMMA but the high quality of the graphene samples were maintained and confirmed based on the high intensity of sp² carbon peaks which mainly contributes to the fitting of the spectra in C1s regions for all the samples. Thus, the oxygen atoms are part of functional groups as C-O, C=O and O-C=O attached to the graphene surface as residues of PMMA, possible defects, bridge of carbon-carbon bonds or at edges.

For the doped samples, the surveys and high resolution spectra presented a peak for potassium which demonstrated the deposition of alkali metal on graphene layer. The functionalization was noncovalent because the sp² carbon peaks were not affected. The

functionalization was produced by cation- π interactions due to electrostatic interaction and induction of energies caused by the positively charged cations and the negatively charged π electron cloud from graphene. In this way, the degree of doping was 30.84% of carbon per potassium based on the atomic percentage of potassium in the analyzed area of K@Gr+H₂O sample (K@Gr+O₂ and K@Gr+Hex could not be measured as it was explained in their subsections) and the highest functionalization degree was 7.63% of carbon per functional group (K@Gr+O₂ sample). Likewise, the samples were n-type doped but due to the oxidation process and formation of functional groups, the graphene samples kept as semiconductor materials without conductive behavior.

From the different environments where the samples were exposed, K@Gr+O₂ sample showed: more oxidation of graphene (20%) due to potassium and O₂ presence, more potassium oxide types as K₂O₂, K₂O₃ and KO₂ and a migration of single bonded oxygen through surface to form potassium oxides. K@Gr+H₂O sample showed: less oxidation of graphene (10%) in H₂O environment and only a type of potassium oxide (K₂O₂). This means that this environment is more stable than the previous and potassium contributes to form specific oxide species. K@Gr+Hex sample showed a sample similar to Gr sample. Its structure was improved and recovered after the doping process. The C1s and O1s spectra show a better quality of graphene without potassium at surface, higher intensity of carbon-carbon peak, less functional groups, less possible defects and with aliphatic chain added to the surface.

As outlook for future research, there are still many open questions that could be developed as quantify the yield for potassium doping and the way of improving the doping process in a homogeneous distribution on samples without PMMA residues, also a project to confirm the potassium iodide salts formation and quantify the recovery of the graphene sample.

Finally, the noncovalent functionalization of graphene is the first approach for changing its inert behavior to make a more soluble and hydrophilic novel structure avoiding defects to maintain the hexagonal structure. The cation doping with functional groups attached to graphene surface can improve the behavior of graphene in order to make a doped semiconductor (reducing the functional groups and PMMA residues attached) suitable for future

applications in electronic devices or more reactive material with other organic solvents (by the functional groups presence) with potential future applications with biomolecules.

- **MWCNTS sample**

The survey and narrow spectra for MWCNTs sample show a highly pure material with the 98.6% of atomic percentage of carbon. The sample also presented a very low concentration of oxygen around 1.2% coming from the decomposition of CaCO_3 substrate but it does not affect the MWCNTs structure. Actually, The C1s spectrum showed that most of the carbon atoms have sp^2 hybridization and metallic behavior as would be expected for MWCNTs. Finally, the MWCNTs were synthesized with high quality without contaminants from the synthesis method which is an advantage to avoid extra processes as purification that might destroy the nanotube structure. Finally, this material can be used as a reference because of its purity and characteristics that help to confirm the functionalization of other samples as graphene.

Appendix A

XPS fitting analysis

In this section, the parameters for the fitting method are presented in order to detail the data used for the peak deconvolution processes for XPS spectra of C1s and O1s region for each one of graphene samples and also for MWCNTs samples. These data was taken from the resulting Origin Pro file after the fitting using Peak Analyzer tool.

C1s fitting - Graphene Pristine						
Peak Index	Peak Type	Area Intg	FWHM	Max Height	Center Grvty	Area IntgP
1	Voigt	4109.92456	0.90955	4244.9712	284.69753	32.25794
2	Voigt	4742.19358	1.2116	3443.84604	285.2053	37.22048
3	Voigt	829.2117	1.56895	483.93177	287.43885	6.50831
4	Voigt	1253.25089	1.7024	584.5402	289.17044	9.8365
5	Voigt	1806.23613	1.50641	1126.41908	286.2775	14.17677
R^2 for fitting = 0.999						

Table A.1: Parameters for the peak deconvolution on C1s region for Gr sample

O1s fitting - Graphene Pristine						
Peak Index	Peak Type	Area Intg	FWHM	Max Height	Center Grvty	Area IntgP
1	Voigt	446.69878	1.68099	239.51232	531.41962	5.11722
2	Voigt	5328.74964	1.52374	3005.19789	532.32837	61.0442
3	Voigt	2953.88084	2.00733	1237.30198	533.50717	33.83858
R^2 for fitting = 0.950						

Table A.2: Parameters for the peak deconvolution on O1s region for Gr sample

C1s fitting - Potassium-doped graphene exposed to air						
Peak Index	Peak Type	Area Intg	FWHM	Max Height	Center Grvty	Area IntgP
1	Voigt	4783.20724	1.42589	2906.10495	284.68998	26.35041
2	Voigt	4203.55052	1.82934	2158.69117	285.45012	23.15712
3	Voigt	2086.29466	2.49349	786.0249	287.43791	11.49328
4	Voigt	330.63331	1.63102	190.43859	289.04479	1.82144
5	Voigt	4449.30844	1.87094	2065.51697	292.71281	24.51098
6	Voigt	2299.30957	2.12857	1014.79056	295.40235	12.66676
R^2 for fitting = 0.998						

Table A.3: Parameters for the peak deconvolution on C1s region for K@Gr+O₂ sample

O1s fitting - Potassium-doped graphene exposed to air						
Peak Index	Peak Type	Area Intg	FWHM	Max Height	Center Grvty	Area IntgP
1	Voigt	275.7448	1.1627	179.15792	529.40305	2.63445
2	Voigt	3134.22825	1.82605	1457.67255	530.95999	29.94422
3	Voigt	4184.4224	1.63006	1993.74457	532.05	39.97771
4	Voigt	2526.77575	1.41473	1293.98231	532.93915	24.14066
5	Voigt	345.7166	1.49465	179.87376	534.3	3.30296
R^2 for fitting = 0.941						

Table A.4: Parameters for the peak deconvolution on O1s region for K@Gr+O₂ sample

C1s fitting - Potassium-doped graphene exposed to water						
Peak Index	Peak Type	Area Intg	FWHM	Max Height	Center Grvty	Area IntgP
1	Voigt	4316.00915	1.05343	3848.9665	284.68828	23.27425
2	Voigt	5020.29804	1.96747	2002.37599	285.35334	27.07215
3	Voigt	1132.46042	1.8216	481.94598	288.34869	6.10684
4	Voigt	5744.1228	1.48277	3089.07819	292.95814	30.97541
5	Voigt	2331.24983	1.46635	1493.54295	295.73501	12.57136
R^2 for fitting = 0.943						

Table A.5: Parameters for the peak deconvolution on C1s region for K@Gr+H₂O sample

O1s fitting - Potassium-doped graphene exposed to water						
Peak Index	Peak Type	Area Intg	FWHM	Max Height	Center Grvty	Area IntgP
1	Voigt	376.80275	1.61934	188.43077	530.10589	4.40579
2	Voigt	2973.47228	1.53365	1610.14699	531.15004	34.76754
3	Voigt	4722.91071	1.5859	2299.36651	532.39186	55.22297
4	Voigt	479.25266	1.05813	323.15264	533.37595	5.6037
R^2 for fitting = 0.935						

Table A.6: Parameters for the peak deconvolution on O1s region for K@Gr+H₂O sample

C1s fitting - Potassium-doped graphene exposed to hexyliodide						
Peak Index	Peak Type	Area Intg	FWHM	Max Height	Center Grvty	Area IntgP
1	Voigt	4245.36802	1.26389	2475.41745	284.5	54.15321
2	Voigt	1305.58727	1.24758	983.1196	285.2	16.65385
3	Voigt	935.83641	1.56697	525.09575	285.91337	11.93737
4	Voigt	566.64181	1.40169	379.46605	287.02955	7.22799
5	Voigt	786.1164	1.70054	434.18972	288.66073	10.02757
R^2 for fitting = 0.949						

Table A.7: Parameters for the peak deconvolution on C1s region for K@Gr+Hex sample

O1s fitting - Potassium-doped graphene exposed to hexyliodide						
Peak Index	Peak Type	Area Intg	FWHM	Max Height	Center Grvty	Area IntgP
1	Voigt	95.86674	0.91775	98.13232	531.09829	1.01852
2	Voigt	8824.68845	1.72696	4040.13133	532.10359	93.75652
3	Voigt	491.79123	1.23909	349.86658	533.40287	5.22496
R^2 for fitting = 0.837						

Table A.8: Parameters for the peak deconvolution on O1s region for K@Gr+Hex sample

C1s fitting - MWCNTs pristine						
Peak Index	Peak Type	Area Intg	FWHM	Max Height	Center Grvty	Area IntgP
1	DoniachSunjic	21853.46739	0.82258	20715.06348	–	60.43868
2	Voigt	4991.13634	2.27307	1720.45809	286.05	13.80365
3	Voigt	7472.68266	6.00361	1015.35729	290.6	20.6667

R^2 for fitting= 0.996

Table A.9: Parameters for the peak deconvolution on C1s region for MWCNTs sample

O1s fitting - MWCNTs pristine						
Peak Index	Peak Type	Area Intg	FWHM	Max Height	Center Grvty	Area IntgP
1	Voigt	1452.661	3.63817	287.3362	532.15	100

R^2 for fitting = 0.912

Table A.10: Parameters for the peak deconvolution on O1s region for MWCNTs sample

Bibliography

- [1] Al-Kharusi, M.; Alzebdeh, K.; Pervez, T. An atomistic-based continuum modeling for evaluation of effective elastic properties of single-walled carbon nanotubes. *Journal of Nanomaterials* **2016**, 2016.
- [2] Corredor, L. *STUDY OF CATALYTIC CONDITIONS FOR THE SYNTHESIS OF CARBON NANOTUBES*; Experimental Faculty of Sciences. University of Zulia. Maracaibo Venezuela., 2015.
- [3] Dai, L. *Carbon nanotechnology: recent developments in chemistry, physics, materials science and device applications*; Elsevier, 2006.
- [4] Feynman, R. P. There's plenty of room at the bottom. *California Institute of Technology, Engineering and Science magazine* **1960**,
- [5] Taniguchi, N. On the basic concept of nanotechnology. *Proceeding of the ICPE* **1974**,
- [6] Pokropivny, V.; Lohmus, R.; Hussainova, I.; Pokropivny, A.; Vlassov, S. *Introduction to nanomaterials and nanotechnology*; Tartu University Press Ukraine, 2007.
- [7] Tagmatarchis, N. *Advances in carbon nanomaterials: Science and applications*; CRC Press, 2012.
- [8] Avouris, P. Graphene: electronic and photonic properties and devices. *Nano letters* **2010**, *10*, 4285–4294.
- [9] Geim, A. K. Graphene: status and prospects. *science* **2009**, *324*, 1530–1534.

- [10] Kuila, T.; Bose, S.; Mishra, A. K.; Khanra, P.; Kim, N. H.; Lee, J. H. Chemical functionalization of graphene and its applications. *Progress in Materials Science* **2012**, *57*, 1061–1105.
- [11] Yan, L.; Zheng, Y. B.; Zhao, F.; Li, S.; Gao, X.; Xu, B.; Weiss, P. S.; Zhao, Y. Chemistry and physics of a single atomic layer: strategies and challenges for functionalization of graphene and graphene-based materials. *Chemical Society Reviews* **2012**, *41*, 97–114.
- [12] Büchner, B.; Pichler, T. Electronic Properties of Functionalized Graphene Studied With Photoemission Spectroscopy. **2012**,
- [13] Raza, H. *Graphene nanoelectronics: Metrology, synthesis, properties and applications*; Springer Science & Business Media, 2012.
- [14] Ren, Z.; Lan, Y.; Wang, Y. *Aligned Carbon Nanotubes*; Springer, 2012; pp 7–43.
- [15] *Nanostructured Materials and Nanotechnology IV: Ceramic Engineering and Science Proceedings, Volume 31*; Ceramic Engineering and Science Proceedings.
- [16] Müller, T. J.; Bunz, U. H. *Functional organic materials: syntheses, strategies and applications*; John Wiley & Sons, 2007.
- [17] Andrade, J. D. *Surface and Interfacial Aspects of Biomedical Polymers: Volume 1 Surface Chemistry and Physics*; Springer Science & Business Media, 2012.
- [18] Moulder, J. F. Handbook of X-ray photoelectron spectroscopy. *Physical electronics* **1995**, 230–232.
- [19] Villa, A.; Dimitratos, N. *Metal-free functionalized carbons in catalysis: synthesis, characterization and applications*; Royal Society of Chemistry, 2018; Vol. 31.
- [20] Axis, K. Peak Fitting in XPS. *Casa XPS* **2006**, 1–29.
- [21] Velo-Gala, I.; López-Peñalver, J. J.; Sánchez-Polo, M.; Rivera-Utrilla, J. Surface modifications of activated carbon by gamma irradiation. *Carbon* **2014**, *67*, 236–249.

- [22] Li, X.-R.; Kong, F.-Y.; Liu, J.; Liang, T.-M.; Xu, J.-J.; Chen, H.-Y. Synthesis of Potassium-Modified Graphene and Its Application in Nitrite-Selective Sensing. *Advanced Functional Materials* **2012**, *22*, 1981–1988.
- [23] Bostwick, A.; Ohta, T.; McChesney, J. L.; Emtsev, K. V.; Speck, F.; Seyller, T.; Horn, K.; Kevan, S. D.; Rotenberg, E. The interaction of quasi-particles in graphene with chemical dopants. *New Journal of Physics* **2010**, *12*, 125014.
- [24] Georgakilas, V.; Otyepka, M.; Bourlinos, A. B.; Chandra, V.; Kim, N.; Kemp, K. C.; Hobza, P.; Zboril, R.; Kim, K. S. Functionalization of graphene: covalent and non-covalent approaches, derivatives and applications. *Chemical reviews* **2012**, *112*, 6156–6214.
- [25] Fedorov, A.; Verbitskiy, N.; Haberer, D.; Struzzi, C.; Petaccia, L.; Usachov, D.; Vilkov, O.; Vyalikh, D.; Fink, J.; Knupfer, M. Observation of a universal donor-dependent vibrational mode in graphene. *Nature communications* **2014**, *5*, 1–8.
- [26] Louette, P.; Bodino, F.; Pireaux, J.-J. Poly (ethyl methacrylate)(PEMA) XPS Reference Core Level and Energy Loss Spectra. *Surface Science Spectra* **2005**, *12*, 44–48.
- [27] Larciprete, R.; Gardonio, S.; Petaccia, L.; Lizzit, S. Atomic oxygen functionalization of double walled C nanotubes. *Carbon* **2009**, *47*, 2579–2589.
- [28] Xie, W.; Weng, L.-T.; Ng, K. M.; Chan, C. K.; Chan, C.-M. Clean graphene surface through high temperature annealing. *Carbon* **2015**, *94*, 740–748.
- [29] Ahn, Y.; Kim, H.; Kim, Y.-H.; Yi, Y.; Kim, S.-I. Procedure of removing polymer residues and its influences on electronic and structural characteristics of graphene. *Applied Physics Letters* **2013**, *102*, 091602.
- [30] Barinov, A.; Malcioglu, O. B.; Fabris, S.; Sun, T.; Gregoratti, L.; Dalmiglio, M.; Kiskinova, M. Initial stages of oxidation on graphitic surfaces: photoemission study and density functional theory calculations. *The Journal of Physical Chemistry C* **2009**, *113*, 9009–9013.
- [31] Borisenko, V. E. *Physics, Chemistry and Applications of Nanostructures: Reviews and Short Notes - Proceedings of the International Conference Nanomeeting - 2011*, 1st ed.; World Scientific Publishing Company, 2011.

- [32] Ren, X.; Zhang, T.; Wu, D.; Yan, T.; Pang, X.; Du, B.; Lou, W.; Wei, Q. Increased electrocatalyzed performance through high content potassium doped graphene matrix and aptamer tri infinite amplification labels strategy: highly sensitive for matrix metalloproteinases-2 detection. *Biosensors and Bioelectronics* **2017**, *94*, 694–700.
- [33] Lamontagne, B.; Semond, F.; Roy, D. K overlayer oxidation studied by XPS: the effects of the adsorption and oxidation conditions. *Surface science* **1995**, *327*, 371–378.
- [34] Klinman, J. P. How do enzymes activate oxygen without inactivating themselves? *Accounts of Chemical Research* **2007**, *40*, 325–333.
- [35] Li, S.; Kang, E.; Neoh, K.; Ma, Z.; Tan, K.; Huang, W. In situ XPS studies of thermally deposited potassium on poly (p-phenylene vinylene) and its ring-substituted derivatives. *Applied surface science* **2001**, *181*, 201–210.
- [36] Dimiev, A. M.; Eigler, S. *Graphene oxide: fundamentals and applications*; John Wiley & Sons, 2016.
- [37] Saha, A.; Basiruddin, S.; Rayb, S.; Royc, S.; Janaa, N. R. Electronic supplementary information Functionalized graphene and graphene oxide solution via polyacrylate coating. *Nanoscale* **2010**, *2*, 2777–2782.
- [38] Ganguly, A.; Sharma, S.; Papakonstantinou, P.; Hamilton, J. Probing the thermal deoxygenation of graphene oxide using high-resolution in situ X-ray-based spectroscopies. *The Journal of Physical Chemistry C* **2011**, *115*, 17009–17019.
- [39] Tetana, Z.; Mhlanga, S.; Bepete, G.; Krause, R.; Coville, N. The synthesis of nitrogen-doped multiwalled carbon nanotubes using an Fe-Co/CaCO₃ catalyst. *South African Journal of Chemistry* **2012**, *65*, 39–49.